DISSERTATIONS IN
FORESTRY AND
NATURAL SCIENCES

Mervi Könönen

Functional Human Neuroimaging Using Clinical Tools

Studies of Cortical Motor Areas

Publications of the University of Eastern Finland
Dissertations in Forestry and Natural Sciences No 208

UNIVERSITY OF
EASTERN FINLAND

MERVI KÖNÖNEN

Functional Human Neuroimaging Using Clinical Tools

Studies of Cortical Motor Areas

Publications of the University of Eastern Finland
Dissertations in Forestry and Natural Sciences
No 208

Academic Dissertation
To be presented by permission of the Faculty of Science and Forestry for public examination in the Auditorium 1 at the Kuopio University Hospital, Kuopio, on 15th January 2016, at 12 o'clock noon.

Diagnostic Imaging Centre, Kuopio University Hospital
Department of Applied Physics

Grano Oy
Kuopio, 2015
Editors: Prof. Pertti Pasanen,
Prof. Pekka Kilpeläinen, Prof. Kai Peiponen, Prof. Matti Vornanen
Distribution:
Eastern Finland University Library / Sales of publications
P.O.Box 107, FI-80101 Joensuu, Finland
tel. +358-50-3058396
http://www.uef.fi/kirjasto

ISBN: 978-952-61-1153-7 (printed)
ISSNL: 1798-5668
ISSN: 1798-5668
ISBN: 978-952-61-1154-4 (pdf)
ISSN: 1798-5676 (pdf)

Author's address:
Kuopio University Hospital
Diagnostic Imaging Centre
P.O.Box 100
70029 KYS, FINLAND
email: Mervi.Kononen@kuh.fi

Supervisors:
Professor Pasi Karjalainen, Ph.D.
University of Eastern Finland
Department of Applied Physics
P.O.Box 1627
70211 KUOPIO, FINLAND
email: Pasi.Karjalainen@uef.fi

Professor Ritva Vanninen, M.D., Ph.D.
Kuopio University Hospital
Department of Clinical Radiology
University of Eastern Finland
School of Medicine, Faculty of Health Sciences
Institute of Clinical Medicine
P.O.Box 1627
70211 KUOPIO, FINLAND
email: Ritva.Vanninen@kuh.fi

Eini Niskanen, Ph.D.
Vaasa Central Hospital
Department of Radiology
Hietalahdenkatu 2–4
65130 VAASA, FINLAND
email: Eini.Niskanen@vshp.fi

Reviewers:
Professor Veikko Jousmäki, Ph.D
Aalto University School of Science
Department of Neuroscience and Biomedical Engineering
P.O.Box 11000
00076 AALTO, FINLAND
email: Veikko.Jousmaki@aalto.fi

Docent Vesa Kiviniemi, Ph.D
University Hospital of Oulu
Department of Clinical Radiology
P.O.Box 50
90029 OYS, FINLAND
email: Vesa.Kiviniemi@oulu.fi

Opponent:

Academy Professor Risto Ilmoniemi
Aalto University School of Science
Department of Neuroscience and Biomedical Engineering
P.O.Box 12200
00076 AALTO, FINLAND
email: Risto.Ilmoniemi@aalto.fi

ABSTRACT

It is very challenging to investigate human brain functions in detail. The execution of one task may involve several brain areas simultaneously functioning as a network, and several tasks can be executed in parallel at the same time.

The goal of this thesis was to investigate the applicability of clinical neuroimaging tools for measuring changes in human brain related to motor functions. Since it is a primary function, motor function and the primary motor (M1) area are suitable targets when undertaking a functional brain examination. Additionally, the cortical motor areas can be localized with several clinical examination methods.

In a longitudinal study, single photon emission tomography (SPET) was utilized to monitor changes in perfusion in the cerebral areas associated with motor function in chronic stroke patients participating in a rehabilitation program. In addition, changes in quantitative functional magnetic resonance imaging (fMRI) and transcranial magnetic stimulation (TMS) parameters were assessed and furthermore the fMRI changes were correlated with the clinical parameters. The fMRI findings highlight the feasibility of developing neuroimaging methods for monitoring the effectiveness of rehabilitation.

Reduced motor activations were detected with a block design fMRI in patients with Unverricht-Lundborg disease in comparison to controls. These fMRI results were in parallel with previous structural and neurophysiological findings and correlated with the severity of the motor symptoms of this disease.

A multimodal approach was used to discern the brain areas responsible to motor and language processes in overt speech production. The reviewer-verified speech disruptions induced by navigated repetitive TMS (rTMS) provided clinically relevant information from both hemispheres. The combination of the localization information from navigated rTMS and the fMRI activation explained further the functions of the cortical areas.

The various clinical neuroimaging tools used in this study appear to be capable of detecting functional changes in those cortical areas related motor functions at the group level. However, further development of the methods will be needed before they are able to detect changes for follow-up or prediction of outcome at the level of individual patient. It is concluded that the adoption of a multimodal approach improves the reliability of mapping of functional areas at the individual level.

National Library of Medicine Classification: WL 141.5.N47, WL 307, WN 185, WN 206

Medical Subject Headings: Diagnostic Imaging; Functional Neuroimaging; Brain; Brain Mapping; Motor Cortex; Cerebrovascular Circulation; Regional Blood Flow; Stroke; Rehabilitation; Unverricht-Lundborg Syndrome; Speech; Tomography, Emission-Computed, Single-Photon; Magnetic Resonance Imaging; Transcranial Magnetic Stimulation

Yleinen suomalainen asiasanasto: kuvantaminen; aivot; aivokuori; verenkierto; aivohalvaus; kuntoutus; Unverricht-Lundborgin oireyhtymä; puhe; tomografia; magneettitutkimus; transkraniaalinen magneettistimulaatio

Acknowledgements

This work was carried out during the years 2001 – 2015 in the Department of Clinical Radiology, the Department of Clinical Physiology, Nuclear Medicine and Clinical Neurophysiology, Kuopio University Hospital and Department of Applied Physics, University of Eastern Finland.

I owe my deepest gratitude to Professor Ritva Vanninen, my supervisor. Her inspiring long-long-lasting confidence and support have made this work possible, and finally borne fruit in the realization of this thesis.

I express my deepest thanks to Physicist Eini Niskanen, Ph.D., my supervisor, for studying and working in the field of neuroimaging together with me. Later while I was writing this thesis, her support and guidance with analysing the fMRI data and scientific writing have been invaluable. I could not have hoped for better supervision.

I am grateful to Professor Pasi Karjalainen, my supervisor and my course colleague. He adapted the academic atmosphere of university so that it could cope with a mature student like me. Additional thanks for these 32 years of being my friend.

I thank the official reviewers Professor Veikko Jousmäki, and Docent Vesa Kiviniemi for their constructive criticism and valuable suggestions they provided to improve the thesis. Ewen MacDonald, Ph.D., is warmly acknowledged for the linguistic revision of the thesis.

I express my warmest thanks to all the co-authors, without whom this work would not have been possible. Clinical research like this thesis, demands expertise from several fields of science. I want thank Docent Ina Tarkka and Professor Juhani Sivenius from Brain Research and Rehabilitation Center Neuron for their collaboration in the stroke studies. I owe my gratitude to Professor Reetta Kälviäinen for integrating me and fMRI to the clinical and molecular genetics study of EPM1. I am grateful to

Päivi Koskenkorva, M.D., Ph.D. for the neuroradiological evaluations of the EPM1 patients. I thank Niko Tamsi, M.D., for his excellent work in rTMS mapping of speech areas. I express my gratitude to Leena Jutila, M.D., Ph.D. and neuro-psychologist Marja Äikiä, Ph.D., for reviewing hundreds of video clips in rTMS study.

I have had a long career in Kuopio University Hospital, a host of co-workers have affected my professional development; some have become lifetime friends. I want thank you all, regardless of the department or year. I owe my gratitude to the personnel of the Department of Clinical Neurophysiology and especially Professor Juhani Partanen and Professor Esa Mervaala for creating such a stimulating and research positive atmosphere. The natives of the NBS unit are cordially acknowledged. I thank the personnel of MRI unit for arranging scanning time for me, and I thank the neuroradiologists for pointing out to me the many mysterious structures in the human brain. I am extremely grateful to my colleagues, my fellow medical physicists in the hospital, my third department, mentioning some by name: Ari, Pauli, Pekka and Petro. Additionally I send my special thanks to Elisa for her peer support.

My dearest thanks to my family and all my friends for sharing the Life with me.

Finally, the gentlemen of my life, Jukka, Konsta, and Juuso, you are my first priority. Our family is fabulous (and loud). The lady of the house has spoken.

This study was financially supported by Kuopio University Hospital (EVO funding 307/97, 21/98; grant numbers 5063503, 5041704, 5772751 and 5041716) and the Radiological Society of Finland.

Kuopio, December 2015

Mervi Könönen

LIST OF ABBREVIATIONS

APB	abductor pollicis brevis
AM	myoclonus action score
BA	Brodmann area
BBB	blood-brain barrier
BOLD	blood-oxygen-level dependent
CIMT	constraint-induced movement therapy
CSF	cerebrospinal fluid
DCS	direct cortical stimulation
EEG	electroencephalography
EMG	electromyography
EPI	echo planar imaging
EPM1	Unverricht-Lundborg disease
FDG	^{18}F-Fluorodeoxyglucose
fMRI	functional magnetic resonance imaging
FWE	familywise error
FWHM	full width at half maximum
GLM	general linear model
GRE	gradient echo
IFJ	inferior frontal junction
LI	laterality index
M1	primary motor
MEG	magnetoencephalography
MEP	motor evoked potential
MPRAGE	magnetization-prepared rapid acquisition gradient-echo
MRI	magnetic resonance imaging
MT	motor threshold
NMR	nuclear magnetic resonance
nTMS	navigated transcranial magnetic stimulation
PET	positron emission tomography
PMA	premotor area
rCBF	regional cerebral blood flow
ROI	region-of-interest
rTMS	repetitive transcranial magnetic stimulation
S1	primary somatosensory

SM1	primary sensorimotor
SMA	supplementary motor area
SNR	signal-to-noise ratio
SPECT	single photon emission computerized tomography
SPET	single photon emission tomography
SPM	statistical parametric mapping
^{99m}Tc	technetium-99m
^{99m}Tc-ECD	^{99m}Tc-ethyl cysteinate dimer
^{99m}Tc-HMPAO	^{99m}Tc-hexamethyl propylene amine oxime
TE	time to echo
TI	inversion time
TMS	transcranial magnetic stimulation
TR	repetition time
WGEN	word generation task
WMFT	Wolf motor function test

LIST OF ORIGINAL PUBLICATIONS

This thesis is based on data presented in the following articles, referred to by the Roman numerals **I – IV**.

I Könönen M., Kuikka J.T., Husso-Saastamoinen M., Vanninen E., Vanninen R., Soimakallio S., Mervaala E., Sivenius J., Pitkänen K., Tarkka I.M. Increased perfusion in motor areas after constraint-induced movement therapy in chronic stroke: a single-photon emission computerized tomography study. *Journal of Cerebral Blood Flow and Metabolism 25: 1668-1674, 2005.*

II Könönen M., Tarkka I.M., Niskanen E., Pihlajamäki M., Mervaala E., Pitkänen K., Vanninen R. Functional MRI and motor behavioral changes obtained with constraint-induced movement therapy in chronic stroke. *European Journal of Neurology 19: 578-586, 2012.*

III Könönen M., Danner N., Koskenkorva P., Kälviäinen R., Hyppönen J., Mervaala E., Karjalainen P., Vanninen R., Niskanen E. Reduced cortical activation in inferior frontal junction in Unverricht-Lundborg disease (EPM1) – A motor fMRI study. *Epilepsy Research 111: 78-84, 2015.*

IV Könönen M., Tamsi N., Säisänen L., Kemppainen S., Määttä S., Julkunen P., Jutila L., Äikiä M., Kälviäinen R., Niskanen E., Vanninen R., Karjalainen P., Mervaala E. Non-invasive mapping of bilateral motor speech areas using navigated transcranial magnetic stimulation and functional magnetic resonance imaging. *Journal of Neuroscience Methods 248:32-40, 2015.*

AUTHOR'S CONTRIBUTION

The publications of this thesis are the result of collaboration between the Departments of Clinical Neurophysiology, Clinical Radiology, Clinical Physiology and Nuclear Medicine, and Neurology, Kuopio University Hospital, Brain Research and Rehabilitation Center Neuron, and the Department of Applied Physics, University of Eastern Finland.

The author's contribution in detail for the publications is as follows:

I The author participated in designing the study plan in collaboration with the co-authors, took care of the logistics of the imaging studies. She was the principal writer of the manuscript.

II The author participated in designing the study plan in collaboration with the co-authors, took care of logistics of the imaging studies, and was responsible for imaging and analysing the fMRI data. She was the principal writer of the manuscript.

III The author designed the fMRI protocol, was responsible for imaging and analysing the fMRI data. She was the principal writer of the manuscript.

IV The author participated in designing the fMRI protocol, acquisition, and analysis of the fMRI data. The author participated also in designing the rTMS protocol and analysis of rTMS data. The author and Niko Tamsi contributed equally to writing of the manuscript.

Contents

1 Introduction 15
2 Anatomy and physiology of motor areas and pathways 19
2.1 Voluntary motor system 19
2.1.1 Motor pathway 20
2.1.2 Action potential 21
2.1.3 Cortical areas of motor functions 23
2.1.4 Cortical areas of language functions 25
2.2 Cortical circulation 25
2.3 Blood-brain barrier 27
2.4 Disturbances in motor function 28
2.4.1 Stroke 28
2.4.2 Unverricht-Lundborg disease 30
3 Functional neuroimaging methods 31
3.1 Single photon emission tomography (SPET) 31
3.1.1 Physiology of cerebral perfusion SPET 32
3.1.2 Cerebral perfusion SPET examination 32
3.1.3 Cerebral perfusion SPET analysis 33
3.2 Functional magnetic resonance imaging (fMRI) 34
3.2.1 Physiology of the BOLD response 36
3.2.2 fMRI examination 38
3.2.3 fMRI analysis 39
3.3 Transcranial magnetic stimulation (TMS) 43
3.3.1 Physiology of TMS responses 43
3.3.2 TMS examination 44
3.3.3 TMS analysis 46
4 Aims of the present study 49
5 Materials and methods 51
5.1 Subjects 51
5.2 Single photon emission tomography (Study I) 53
5.2.1 Cerebral perfusion SPET examination 53
5.2.2 Cerebral perfusion SPET analysis 54

5.3 Functional magnetic resonance imaging (Studies II, III, and IV) 54
5.3.1 fMRI and MRI examinations *54*
5.3.2 fMRI analysis *56*
5.4 Transcranial magnetic stimulation (Studies II and IV) 59
5.4.1 TMS examination *59*
5.4.2 TMS analysis *61*
5.5 Statistical tests 63
5.6 Additional methods 63
5.6.1 Constraint-induced movement therapy (CIMT) (Studies I and II) *63*
5.6.2 Structured motor function test (Studies I and II) *64*
6 Results 65
6.1 Functional changes in motor related cortical areas induced by CIMT in stroke patients (Studies I and II) 65
6.1.1 Motor functions *65*
6.1.2 Cerebral perfusion SPET results *65*
6.1.3 fMRI results *67*
6.1.4 TMS and its correspondence with fMRI *69*
6.2 Altered motor activation in EPM1 patients (Study III) 70
6.3 Mapping of motor speech areas using navigated rTMS and fMRI in healthy volunteers (Study IV) 71
6.3.1 Speech disruptions with rTMS *71*
6.3.2 Combination of navigated rTMS and fMRI *72*
7 Discussion 75
7.1 Detection of changes in functionality of motor area in stroke patients 75
7.2 Altered motor activation in EPM1 patients 77
7.3 Separation of motor speech areas from language areas in healthy volunteers 78
7.4 Future aspects 79
8 Conclusions 81
References 83

Introduction

Nowadays, the imaging of human brain anatomy with magnetic resonance imaging (MRI) and computed tomography are basic diagnostic tools in clinical radiology. MRI offers the best spatial resolution for diagnostics, it also offers superior contrast between cerebral grey and white matter and between focal abnormalities and normal parenchyma. Although the human brain is a complex organ, it can be defined by anatomical areas, e.g. lobes and structures, functional areas, as well as via its cytoarchitecture which are designated as Brodmann areas (BA) [20, 56]. Several brain areas need to participate in the execution of even one simple task as a network, and furthermore, several tasks can be executed in parallel. Thus it is challenging to investigate brain functions in detail.

Neuroimaging is important both in clinical medicine and in basic research. In research, experimental methods, such as invasive stimulations or recordings, can be used together with time consuming calculations or analysis. In diagnostic work, however, the methods need to be non-invasive, risk-free, cost-effective, and feasible to perform in hospital environment.

When planning or performing neurosurgical resection, it is crucial that one can make accurate identifications of eloquent areas of motor, sensory, and language functions. Functional neuroimaging methods are clinically used also for the diagnosis of brain diseases such as metabolic disorders, stroke, other cerebrovascular disorders, neurodegenerative diseases, and inflammation.

Clinical tools for functional neuroimaging give rise to various kinds of images and recordings for diagnostics. Electrical brain activity can be recorded by electroencephalography (EEG) or magnetoencephalography (MEG). These methods measure neural activity directly. Brain perfusion changes linked to a performed task, or brain perfusion at rest can be examined by

functional magnetic resonance imaging (fMRI), single photon emission tomography (SPET), and positron emission tomography (PET). However, these methods are indirect measures of neural activity. The direct methods have a better temporal resolution compared to indirect methods. The advantages of indirect methods are related to their better spatial resolution. Furthermore, functional brain areas can be examined with transcranial magnetic stimulation (TMS) by stimulating the cortex thus eliciting primary responses or interfering the task performance. The availability of MEG and PET is limited as a result of high costs or demanding technical issues.

Motor function and the primary motor (M1) area are suitable targets for functional neuroimaging. A motor response, muscle movement, is visible, easy to measure, and simple to control as a task. In addition to the M1 area, the motor network commonly includes the premotor area (PMA) and the supplementary motor area (SMA), which together play a dominant role in the planning, specification and execution of action. The activation of the cortical motor areas can be localized with fMRI, PET, EEG, and MEG. The M1 area can be activated by TMS, and when used with on-line navigation utilizing individual MRIs, also the anatomical locations of the stimulated sites can be defined. The accuracy of localizing methods can be estimated by comparing the result with the so-called golden standard, direct cortical stimulation (DCS) in craniotomy [161]. Reliable localization results have been reported for fMRI [12, 98], navigated TMS (nTMS) [51, 89, 133] and PET [149]. The nTMS has been proven to be more accurate than fMRI when compared to DCS, deviations are around 10 mm between nTMS and DCS, and about 14 mm between fMRI and fMRI [51, 106].

The mapping of speech and language areas is more challenging than the mapping of motor areas. The functional neuroanatomy of speech processing has been difficult to characterize since it utilizes several parallel and simultaneously processing networks [65]. Speech production requires activation of the motor cortices and also the integration and coordination between multiple brain regions associated with various speech-

related processes, such as auditory perception, semantic processing, memory encoding, and preparation for motor execution [150]. However, a study conducted on patients with lesions in language-eloquent regions have shown that language function mapping with navigated repetitive TMS (rTMS) correlates well with intraoperative DCS [131]. fMRI with word-generation tasks (WGEN) produces accurate maps of Broca's area which is responsible for planning and executing speech, and these fMRI maps coincided reliably with DCS localization in awake craniotomy [17].

In order to measure accurately physiological or pathological alterations in cortical functionality with clinical neuroimaging methods, the reproducibility of the chosen method between two sessions should be acceptable to allow the detection of the changes in function of the target area. The reproducibility of fMRI between runs and sessions has been reported consistently as being much greater for single individuals than between individuals [16]. Although fMRI has showed moderate to good reliability between sessions conducted in stroke patients performing a visual motor task [81], poor repeatability of quantitative fMRI parameters has been reported in healthy elderly volunteers [108].

The average intra-subject reproducibility in brain perfusion in SPET has been shown to be 3.0 % (range 1.4 % – 6.2 %), when the reproducibility was defined as the average of the absolute value of the intra-individual differences obtained from two scans [176]. Furthermore, inter-subject variability appears to be small in regional SPET brain perfusion patterns in healthy adults [164, 176].

The TMS-related measure, i.e. latency and amplitude of motor evoked potentials (MEP) and resting motor threshold (MT), have been demonstrated to be reliable in healthy subjects and in patients with chronic stroke [24].

The goal of this research was to investigate the feasibility of clinical neuroimaging tools to study function of cerebral areas which participate in the execution of motor tasks. In a longitudinal study on chronic stroke patients in a rehabilitation

program, SPET, fMRI, and TMS were used to detect functional changes in motor area (Studies **I** and **II**). In a cross-sectional study on patients with Unverricht-Lundborg disease (EPM1), fMRI was utilized to detect altered motor activation related to the impaired motor performance (Study **III**). In a multimodal approach, the separation of motor speech areas from language areas was studied combining rTMS and fMRI (Study **IV**).

2 Anatomy and physiology of motor areas and pathways

2.1 VOLUNTARY MOTOR SYSTEM

Neurons in the M1 area, the region of the human brain that executes voluntary movements, send their axons through the corticospinal tract to connect with motor neurons in the spinal cord. Supplementary and premotor cortical areas are responsible for the planning and preparation for movement, see Figure 2.1. The spinal motoneurons project out of the cord to the muscles via the ventral root.

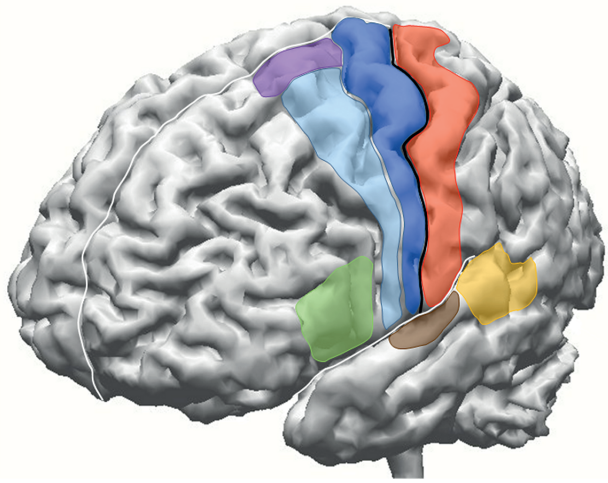

Figure 2.1: *A schematic figure of cortical motor and language areas. Primary motor area (marine blue) is located on the anterior wall of the central sulcus, extending anteriorly from the sulcus partly onto the precentral gyrus. Supplementary (purple) and premotor cortical (light blue) areas are anterior to M1 area. Primary somatosensory (red) area is located on postcentral gyrus. Broca's area (green) is the expressive area for executed speech, Wernicke's area (yellow) is the receptive speech area, and Heschl gyrus (brown) is the primary auditory cortex participating also in speech tasks. The central sulcus is enhanced with the black line.*

2.1.1 Motor pathway

The M1 area is a brain region located in the posterior portion of the frontal lobe, on the anterior wall of the central sulcus, extending anteriorly from the sulcus partly onto the precentral gyrus. In the lateral direction, the M1 area is bordered by the insular cortex in the lateral sulcus, and it extends medially to the top of the hemisphere and then continues onto the medial wall of the hemisphere.

The neocortex has a common basic structure, with neurons arranged in six layers, or laminae, oriented parallel to the surface of the cortex, numbered from the most superficial layer 1 to the deepest multiform layer 6 [19, 56]. Layers 3 and 5 contain pyramidal cells: the external pyramidal layer (3) and the internal pyramidal layer (5) [19]. The cortical output is mediated through pyramidal neurons, which are highly polarized with a major orientation axis perpendicular to the pial surface of the cerebral cortex [68]. In the M1 area, layer V contains giant pyramidal cells, Betz cells, whose axons travel through the internal capsule, the brain stem and the spinal cord forming the corticospinal tract, known as pyramidal tract, which is the main pathway for voluntary motor control [68].

The pyramidal tract is crucial for an individual to be able to perform precise voluntary movements. The majority of the fibres of the pyramidal tract originate from Betz cells in M1 area, the rest of the fibres come from the premotor area, supplementary motor area, and sensory areas [29, 138]. At the decussation of pyramids, most of the corticospinal fibres cross the midline and continue in the lateral funicle of the cord [29]. Some of the efferent pyramidal tract fibres from the M1 area end monosynaptically on the lower motoneurons [19, 170]. Monosynaptic connections are important for movements that require the highest degree of voluntary control [19]. The lower motoneuron's axon innervates the motor endplate, a specialized area of the muscle membrane, and releases the neurotransmitter acetylcholine at a synapse, called the neuromuscular junction [80]. See Figure 2.2 for the schematic illustration of the motor pathway. Acetylcholine binds to cholinergic nicotinic receptors

on the muscle fibre, and triggers the contraction of the muscle [19, 80].

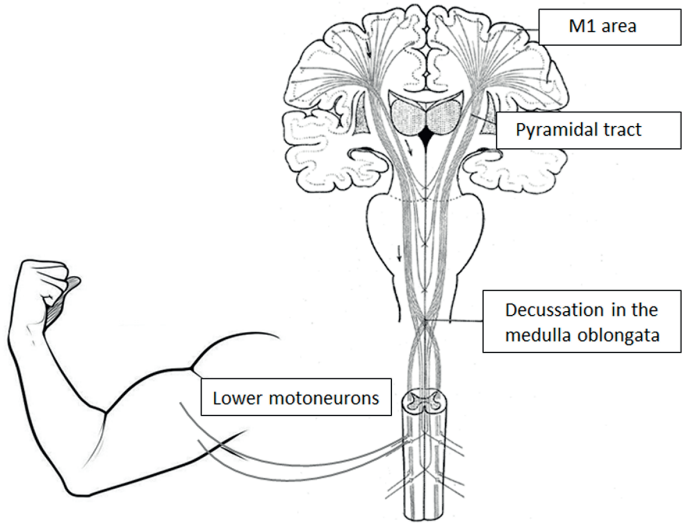

Figure 2.2: *Motor pathway. The majority of the pyramidal tract originates from the M1 area. At the decussation of pyramids, most of the corticospinal fibres cross the midline and continue in the lateral funicle of the cord. Pyramidal tract is connected synaptically to lower motoneurons whose axons innervate the motor endplates in muscle.*

2.1.2 Action potential

The ability of nerve cells to carry a signal over long distances is based on action potentials moving along the axons which do not attenuate as they move away from their site of initiation [83]. In a typical nerve cell in the resting state, the potential across the cell membrane is stable at around -60 mV [111]. The inner side of the membrane is negatively charged in comparison with the outside, due to a small surplus of anions inside the cell [19, 111]. The intracellular and extracellular concentrations of Na^+, K^+, Cl^- and Ca^{2+} differ markedly [111]. The cell membrane is almost impermeable to ions other than K^+. The voltage gradient across the membrane drives K^+ ions inside the cell and at the same time, the concentration gradient drives K^+ ions outside [19]. At the equilibrium potential for K^+ (-75 mV), these two forces are equal, the resting potential in most neurons (from -75 mV to -45

mV) is lower because the cell membrane is almost impermeable to Na^+ [19].

An abrupt increase in Na^+ and K^+ conductance triggers the action potential [111]. The basis of action potential is attributable to the presence of voltage-gated Na^+ channels, the opening of the channels requires the depolarization of membrane to a certain threshold value [19]. Depolarization is induced either by the actions of neurotransmitter acting on neurotransmitter-gated channels, or artificially by direct electrical stimulation. When the voltage-gated channels have been opened, Na^+ flows into the cell driven by both the concentration gradient and the membrane potential. The result is that the membrane becomes more depolarized, and this induces more voltage-gated channels to open further along the membrane. The inward current of Na^+ ions stops when the membrane becomes depolarized to +55 mV. At that value, the inward force caused by the concentration gradient is equal to the outward electrical force and the membrane again become impermeable to Na^+. In this situation with a positive membrane potential, K^+ is driven out by both the concentration gradient and the membrane potential generating a net outward flow of positive charges. There are additional voltage-gated K^+ channels which speed up the recovery. This recovery of potential is termed as the repolarization of membrane. The interior of the cell becomes even more negative than at resting potential, resulting in hyperpolarization. Between each action potential and during rest, there is active pumping to ensure that Na^+ is moved out and K^+ is transported in; a process undertaken by the sodium-potassium pump and ultimately the membrane potential reaches its resting potential. The action potential usually arises in the initial segment of axon: if the depolarization is sufficiently strong, voltage-gated Na^+ and K^+ channels open and trigger an action potential that is propagated along the axon. In a typical nerve, an action potential lasts about 1 ms. The principle of the action potential is described based on [19]. Figure 2.3 illustrates the action potential graphically.

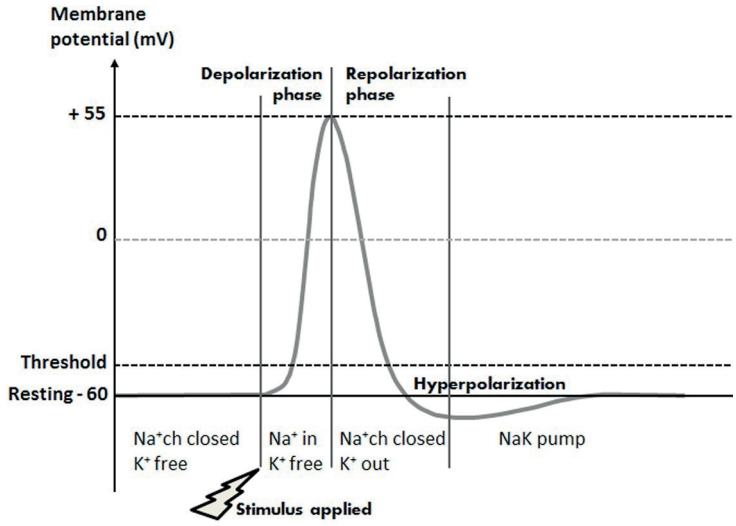

Figure 2.3: *A schematic illustration of the action potential, the sequence of depolarization-repolarization takes generally 1 ms to 2 ms in neuron.*

2.1.3 Cortical areas of motor functions

At the M1 area, the motor representation is somatotopically organized along the central sulcus from the foot (at the medial wall of the cerebral hemisphere) to tongue (close to lateral sulcus), see Figure 2.4 originally described by Penfield [130]. The amount of cortical neurons related to the motor control of a particular body part depends on the variety and precision of the movements rather than on the size of the body part [19, 148]. A disproportionally large part of the M1 area is devoted to control of the hand, lips, and tongue [19]. The M1 area of one hemisphere contains motor representation of the opposite (contralateral) side of the body. The muscles of the head generally receive both crossed and uncrossed pyramidal tract fibres [19].

In addition to the M1 area, many other cortical areas are actively related to movement. A simple finger-movement task activates SMA, PMA and the primary somatosensory (S1) area of the hand in addition to M1 area [148]. The SMA is located in front of the M1 area on the medial site of the hemisphere [19]. The neuronal activity in the SMA when the subject performs complex movements [19], and SMA is involved in the

preparation and planning of movements [172]. The premotor area lies anterior to M1 area and laterally from SMA. PMA activity is associated with complex motor performance and motor learning [129]. The S1 area is located on the postcentral gyrus, and it has somatotopy similar to the M1 area. The S1 area plays a critical role in processing the afferent somatosensory input and it contributes to the integration of sensory and motor signals necessary for skilled movement [15]. Brodmann areas 1, 2, and 3 form the S1 area. BA 3b receives sensory signals from muscle spindles and BA 2 is influenced by proprioceptors to a larger extent that BA 3b [19]. The primary signals from the proprioceptors are conveyed to the motor area. Proprioceptive feedback and the connections from the S1 area to M1 area are particularly important while executing precise movements and learning new movements [19]. See Figure 2.1 for the locations of the motor and sensory areas.

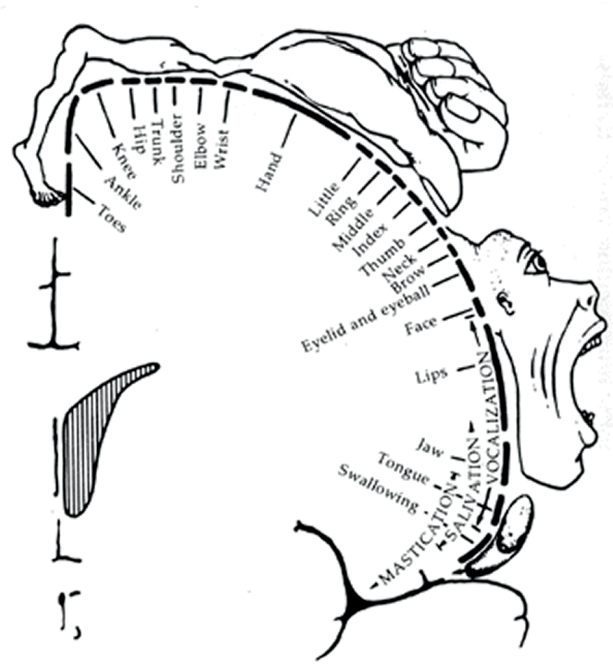

Figure 2.4: *A cortical homunculus is a pictorial representation of the anatomical divisions of the primary motor area described by Wilder Penfield in the 1930s. The figure is according to "The motor and sensory homunculus: the first map". Penfield and Rasmussen, 1950 [130].*

2.1.4 Cortical areas of language functions

Speaking is a complex motor action, the brain has to coordinate the movement of respiratory, laryngeal, articulatory and facial muscles in order to produce speech sounds [8]. Thus, the production of a spoken word requires not only activation of the motor cortices but also integration and coordination between the multiple brain regions associated with various speech-related processes, such as auditory perception, semantic processing, memory encoding, and preparation for motor execution [150]. One classical model of language organization is based on data from aphasic patients with brain lesions: a frontal, "expressive" area for planning and executing speech and writing movements, named after P. Broca [18], and a posterior, "receptive" area for analysis and identification of linguistic sensory stimuli, named after C. Wernicke [11, 185] (see Figure 2.1). The arcuate fasciculus connects these two important areas for language use [25].

About 95% of right-handed individuals have left hemisphere language dominance, whereas the corresponding value for left-handers is about 70% [19]. The growing consensus is that the language faculty is supported by distributed, large-scale cortical, and subcortical networks. Most models of perisylvian connectivity propose that there is a dual (dorsal, ventral) architecture for language, in which a dorsal stream is thought to be involved in mapping auditory speech sounds to articulatory (motor) representations, and a ventral stream which maps auditory speech sounds to meaning, but the function and connectivity of both pathways remains controversial [43]. The primary auditory area is located on the Heschl gyrus and it has connections with both the Broca's and Wernicke's areas [126].

2.2 CORTICAL CIRCULATION

The human brain receives about 15% of the cardiac output and consumes approximately 20% of the oxygen used by the entire body [21]. The average resting blood perfusion in the brain is

50ml/min/100g. Most of this flow is directed to the cerebral grey matter, which has a high energy demand [87]. The middle cerebral artery supplies the motor and somatosensory cortical areas, except for their most medial parts (lower limb area), which are fed by the anterior cerebral artery [19]. Blood vessels form an extremely rich network in the central nervous system, particularly in the cerebral cortex and subcortical grey matter. Within the cerebral grey matter, penetrating arteries divide into a large number of small arterioles that eventually form a highly anastomotic capillary bed. There are venules at the other end of the capillary network, drain into the larger cerebral veins [68].

The cerebral circulation has a high degree of autoregulation, meaning that conditions within the brain itself adjust the blood flow. Cerebral autoregulation is a homeostatic mechanism that minimizes deviations in cerebral blood flow when cerebral perfusion pressure changes; this acts through vasomotor effectors that control cerebrovascular resistance [1]. Local changes in the immediate surroundings of the neurons, like concentrations of CO_2 and O_2 molecules, have an important role in cerebral circulation [19]. The cerebral blood perfusion plays a key role in the transportation of oxygen and nutrients to the brain and is tightly coupled with brain metabolism. This close coupling allows regional brain function to be assessed through measurements of regional cerebral blood flow (rCBF) [139] which is also used to map changes in regional brain function in response to task [37]. Even in hyperoxic or hyperglycemic states, the brain exhibits functional hyperemia in response to stimulation despite plentiful availability of oxygen and/or glucose as shown in rat studies [102, 189], suggesting that the increased blood flow is not triggered simply by local depletion of nutrients. The underlying purpose of functional hyperemia is still unresolved, but a range of cellular mechanisms, including astrocytes, pericytes, and interneurons, have been proposed to play a role in functional neurovascular coupling [66, 67].

2.3 BLOOD-BRAIN BARRIER

Brain capillaries contribute to a distinct function called the blood-brain barrier (BBB) [87], which is critical for neuronal function since it maintains a constant intracerebral milieu [68]. It supplies the brain with essential nutrients and mediates the efflux of many waste products [2]. The structural characteristics of neural capillaries create a barrier to simple diffusion of substances between the blood and the brain extracellular space; only uncharged, lipophilic molecules can diffuse across the brain endothelium. For example, radiopharmaceuticals for the brain perfusion studies are diffusible tracers, which are passively diffused across an intact BBB [83].

The BBB is composed of three cellular components – endothelial cells, pericytes, and astrocytes – and one noncellular component, the basement membrane. These components interact with each other to produce a highly selective and dynamic barrier system [68]. The intercellular junctions between endothelial cells are tightly apposed and this limits the free flow of substances but permits the passage of uncharged, lipid-soluble molecules. The basement membrane is continuous and restricts simple diffusion processes. The paucity of pinocytic vesicles prevents transport of high molecular weight substances [87]. The tight junctions between adjacent endothelial cells force most molecular traffic to take a transcellular route across the BBB. There are several brain endothelial transporters that supply the brain with nutrients e.g. the glucose carrier, several amino acid carriers, and transporters for nucleosides, nucleobases, and many other substances [2]. Astrocytes are in close contact with neurons, capillaries, and the cerebrospinal fluid. They contribute to brain homeostasis in several ways including upregulation of many BBB features, inducing and maintaining the tight junctions in endothelial cells [2]. The transport of specific nutrients into the brain is regulated by BBB transport proteins distributed according to the regional and metabolic requirements of the brain tissue [68]. In recent studies, a glymphatic system has been defined as a brain-wide

paravascular pathway for cerebrospinal fluid and interstitial fluid exchange that facilitates efficient clearance of solutes and waste from the brain [74, 157].

Several types of brain injury, such as ischemic, hemorrhagic, traumatic, inflammatory, and neoplastic disorders can lead to dysfunction and further breakdown of BBB. A dysfunction of BBB can be associated with the loss of neuronal tissue and altered permeability may affect the passage of drugs or contrast material to the brain parenchyma.

2.4 DISTURBANCES IN MOTOR FUNCTION

2.4.1 Stroke

A stroke is a "brain attack". It occurs either when the blood supply to a certain region of the brain is blocked causing ischemia or there is an intracranial hemorrhage. In ischemic stroke, brain cells are deprived of oxygen and begin to die. There are three currently recognized mechanisms which can lead to an ischemic stroke are embolism, decreased perfusion, and thrombosis [192]. An embolism in the brain can be arterial or cardiac in origin, with atrial fibrillation being by far the most common cause of cardioembolic stroke [32, 49].

Every year about 16.9 million people worldwide suffer a first stroke, and about 33 million stroke survivors and 5.9 million stroke-related deaths have been reported [46]. The majority, 80% of the survivors have motor impairments of the upper limb [96]. Ischemic stroke is one of the leading causes of long-term disability in adults: motor impairments, including hemiparesis, incoordination, and spasticity are the most common deficits. During the recovery after a stroke, the surviving brain regions become reorganized to make the most efficient use of the remaining networks [182]. Most patients recover at least some of their lost motor function over time, though the degree of this recovery is variable [146]. This spontaneous recovery starts within the first days post-stroke and it proceeds for several weeks. The chronic phase of stroke begins weeks to months after

an acute stroke when spontaneous recovery has reached a plateau and represents a stable but still modifiable state [62].

Neuroplasticity is defined as the ability of the brain to change its structure and/or function in response to internal and external constraints and goals [84]. Cortical plasticity in the motor area may rely on one or more of the following mechanisms: unmasking of existing but functionally weak synaptic connections by intracortical facilitation or inhibition, strengthening or weakening of existing connection by long-term potentiation or depression, generalized modulatory effects with pharmacological changes, and neurogenesis or synaptogenesis [123]. Studies conducted in primates have shown that motor neuroplasticity is dependent on limb use, both in intact monkeys [120] and in monkeys after ischemic damage [121]. A repetitive motor movement alone, without the need for learning, may not achieve a functional reorganization of the cortical map [134]. Secondary motor areas are involved in remodeling processes initiated by lesions to the M1 area, not only in the ipsilesional hemisphere but also in the contralesional hemisphere [69].

Most stroke rehabilitation protocols are based on motor training to induce neural plasticity, which refers to the ability of the brain to develop new neuronal interconnections, acquire new function, and to compensate for impairment [162].

Constraint-induced movement therapy (CIMT) or modified versions of CIMT are considered as the most effective treatment regimens in physical therapy to improve outcome of the upper paretic limb [93, 95, 177]. The CIMT consists of intensive, graded practice of the paretic upper limb for up to 6 hours a day for 2 weeks. The therapy involves restraint of the contralateral upper limb by means of a splint, mitt and/or sling during most of the therapy period [166]. Stroke patients participating in CIMT manifest learned nonuse of the paretic upper limb. One important inclusion criterion is that patients show voluntary extension (at least 10 to 20°) at the wrist and minimal extension of 10° at the metacarpophalangeal and interphalangeal joints at baseline [166, 188].

2.4.2 Unverricht-Lundborg disease

Unverricht-Lundborg disease (EPM1) is the most common form of the progressive myoclonus epilepsies. It is an autosomal recessively inherited disorder caused by mutations in the cystatin B gene [100]. EPM1 is characterized by stimulus-sensitive and action-activated myoclonus, tonic-clonic seizures, and ataxia. Although the epileptic seizures can be relatively well managed with anti-epileptic medications, the myoclonus is much more resistant to treatment [79], and thus it is the most incapacitating symptom of the disease. Some patients may experience only mild difficulties in performing motor tasks, whereas others may become wheelchair-bound and dependent on others for help with daily routines due to almost continuous myoclonus. The course of the disease is initially progressive during the first 5 years – 10 years after onset, although the symptoms may stabilize thereafter [48].

The baseline EEG activity varies from normal to mildly slowed in EPM1 patients [99]. The changes in the reactivity of EEG have been associated with alterations in the activity and inhibition of motor area [178, 179]. Furthermore, an inhibitory tonus of the M1 area and a lack of normal cortical plasticity are typically encountered [33, 35]. In addition, the alterations in cortical excitability have been reported to correlate with the clinical severity of the symptoms [34]. Despite the pronounced motor symptoms and signs in EPM1, at the time of diagnosis it is rather common that one cannot detect any brain abnormalities in the patients if one conducts a structural MRI. In a group level analysis, some atrophic findings have been discovered in sensorimotor (SM1) areas in comparison to healthy controls [85, 86].

3 Functional neuroimaging methods

3.1 SINGLE PHOTON EMISSION TOMOGRAPHY (SPET)

The nuclear reactor facilities that were developed as part of the Manhattan Project at the end of Second World War started to be used for the production of radioactive isotopes in quantities sufficient for medical applications [28]. The rectilinear scanner was developed as a combination of a scintillation detector and mechanical scanning apparatus in 1951 by B. Cassen to record the two dimensional distribution of a radio-pharmaceutical in a patient [136]. Two dimensional images were scanned for the first time with the Anger camera in 1958 [3], H. Anger's key insight was that the location of a gamma ray interaction could be determined by the distribution of scintillations of light among many photomultiplier tubes [136]. The introduction of technetium-99^{m} (^{99m}TC) as a radiotracer agent into clinical practice in 1964 by P. Harper was a major turning point in the development of nuclear medicine [28]. During the 1970s the reconstruction of tomographic images from a set of angular views around the patient allowed the replacement of two-dimensional imaging with three-dimensional imaging, and the modern era of nuclear medicine began [28].

SPET, also known as single photon emission computerized tomography (SPECT), is a nuclear medicine tomographic imaging technique exploiting radionuclides that emit gamma rays. A SPET study involves injecting a compound (called a radiopharmaceutical, a tracer or a radiotracer), which is a carrier molecule labelled with a gamma-ray-emitting radionuclide, into the body. The carrier molecule is chosen according to the target organ and function. When the radionuclide decays, gamma radiation is emitted. The radiation is detected with an external

gamma camera. The most frequent use of SPET has been in studies of myocardial perfusion but also cerebral perfusion studies have been conducted frequently. Another important application of SPET is in oncology, tracers will be accumulated in cancerous cells and thus reveal the presence of the malignancy. Other areas in which SPET in utilized include imaging of infection and inflammation, and measurement of kidney and liver function [28].

3.1.1 Physiology of cerebral perfusion SPET

A radiopharmaceutical can be defined as a chemical substance that contains radioactive atoms within its structure and is suitable for administration to humans for either the diagnosis or treatment of disease [87]. Radiopharmaceuticals for central nervous system evaluation can be divided into five main groups: non-diffusible tracers, diffusible tracers, metabolism markers, cerebrospinal fluid agents, and receptor imaging agents. In the rCBF studies, diffusible tracers are used. These tracers are neutral lipophilic complexes that passively diffuse through the endothelial cells of the brain's capillaries i.e. they can pass through an intact BBB [87]. The tracers, ^{99m}Tc-hexamethyl propylene amine oxime (^{99m}Tc-HMPAO), also known as ^{99m}Tc-exametazime, and 99mTc-ethyl cysteinate dimer (^{99m}Tc-ECD), also known as ^{99m}Tc-bicisate, cross the blood-brain barrier with rapid first-pass uptake in proportion to rCBF, with slow clearance. Once within the brain tissue, ^{99m}Tc-HMPAO is metabolized into a hydrophilic form and ^{99m}Tc-ECD undergoes de-esterification to a polar metabolite, which is not able to recross the BBB [114].

3.1.2 Cerebral perfusion SPET examination

^{99m}Tc-ECD and ^{99m}Tc-HMPAO are injected intravenously using dose of 370 MBq to 740 MBq. Sensory stimuli such as pain, noise, light, or patient motion affect rCBF and are therefore minimized at the time of injection to prevent interfering increased activity in the corresponding sensory area.

SPET scans are obtained about 10 minutes (^{99m}Tc-HMPAO) or 45 minutes (^{99m}Tc-ECD) after injection. Data are collected from many angles around the patient as two dimensional images (also called projections) and cross-sectional images of the radionuclide distribution are reconstructed from the projections [28]. The attenuation of gamma-rays within the body, scattered radiation and collimator correction are taken into account in the modern reconstruction algorithms. The spatial resolution of the entire camera system is related factors such as the collimator resolution, septal penetration, and scattered radiation. When state-of-the-art cameras and ^{99m}Tc are used, the spatial resolution can be between 3 mm – 5 mm [114].

PET is another nuclear medicine tomographic imaging technique. PET is using positron emitters as the radionuclide. An emitted positron becomes annihilated when it encounters an electron. The annihilation generates two 511 keV gamma photons, which are emitted in opposite directions at about a 180° angle from each other, coincidentally reaching the PET detectors within a time window of 6 ns to 12 ns [114]. ^{18}F-fluorodeoxyglucose (FDG) is a glucose analog which reflects regional glucose metabolism in tissue. The short half-life of PET tracers restricts the use of PET: FDG has a half-life of 110 minutes and that of O-15 is a mere 2.1 minutes.

3.1.3 Cerebral perfusion SPET analysis

In a typical regional cerebral perfusion SPET image, activity is symmetric and strongest in the cortex along the convexity of the frontal, parietal, temporal, and occipital lobes [114]. However, in quantitative analyses of ^{99m}Tc-ECD, tracer uptake without hemispheric differences [164], and overall asymmetry towards the right hemisphere [176] have been discovered. Activity accumulates in the regions corresponding to subcortical grey matter, including the basal ganglia and the thalamus. The regional cerebral perfusion images should be inspected for symmetry of radiopharmaceutical distribution and for continuity of perfusion in the rim of cortical grey matter [114].

The cerebral perfusion SPET is useful mainly in the diagnosis of cerebrovascular diseases. Figure 3.1 shows an age matched pair of subjects, one having suffered a stroke and one with normal cerebral perfusion. SPET is used also in diagnosis of neurodegenerative diseases, encephalitis, and localizing of epileptic focus. Usually the SPET images are inspected together with computed tomography or MR images. Nowadays brain perfusion SPET is often replaced with FDG PET, if possible.

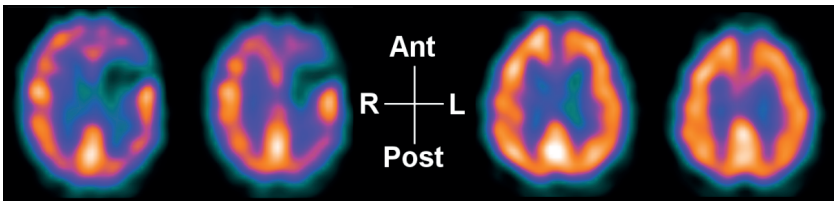

Figure 3.1: *SPET images of an 80 year-old male with left frontal infarction (left). SPET images of a 79 year-old male with normal perfusion (right). Images are in radiological orientation.*

3.2 FUNCTIONAL MAGNETIC RESONANCE IMAGING (FMRI)

In 1937, it was recognized that atomic nuclei were able to absorb and emit radio waves when exposed to a sufficiently strong magnetic field. This phenomenon is known as nuclear magnetic resonance (NMR). In 1946, the magnetic resonance properties of atoms and molecules in solids and liquids were discovered independently by E. Purcell [137] and F. Bloch [14]. This discovery enabled examination of molecular structure of compounds. The spatial localization of the MR signal by using gradients was developed by P. Lauterbur [97] and P. Mansfield [107] independently in the mid-1970s. Subsequently, the first live human subject was imaged in 1977 by R. Damadian. MRI scanners became commercially available in the 1980s, and are now commonly used for imaging the human body.

The signal intensity in the MRI is dependent on proton density and properties of protons to recover after the initial radio frequency pulse. By changing the imaging parameters in

the scanning pulse sequences, the contrast of MRI changes accordingly. In a T1-weighted brain MRI, cerebrospinal fluid (CSF) is dark, fat is bright and white matter is brighter than grey matter. The good contrast between white and grey matter means that the T1-contrast is excellent for anatomical imaging. In T2-weighted brain MRI, CSF is bright and grey matter brighter than white matter. The bright fluid contrast means that T2-weighted MRI is sensitive at detecting pathological processes. T2*-weighted images show local magnetic field inhomogeneities as being dark, a property that has been utilized in imaging of tissues with dissimilar magnetic susceptibilities, such as imaging of hemorrhages, calcification, and iron deposition in various tissues.

Brain activity can be detected by fMRI based on changes in cerebral blood flow related to neuronal activation. The most commonly used form of fMRI uses the blood-oxygen-level-dependent (BOLD) contrast which was discovered S. Ogawa [122]. The first functional magnetic resonance maps of human task activation were published by J. Belliveau and colleagues in 1991 [9]. Arterial spin-labelled perfusion MRI can also be used for functional imaging [36]. The major advantages of fMRI are that it is non-invasive and does not use ionizing radiation. It has also good spatial resolution compared to nuclear medicine tomographic imaging techniques. These features have made fMRI a widely used neuroimaging technique in research. In diagnostics, fMRI is used for localizing cerebral areas of primary functions, such as the motor and visual areas, and also language related areas [10, 175].

During an fMRI experiment, images are collected as a time series while the subject is performing the task, or in the resting state without a task. If the signal intensity of the voxel time series is synchronized with the task, those areas are presumed to be activated by the task. In the resting state fMRI, synchronous fluctuation in fMRI signal between brain areas and brain connectomes are studied.

3.2.1 Physiology of the BOLD response

The physical basis of the BOLD sensitivity of the MR signal is that deoxyhemoglobin alters the magnetic susceptibility of blood. Magnetic susceptibility is a quantitative measure of a material's tendency to interact with and distort an applied magnetic field [147]. This distortion shortens the T2* relaxation time which is seen as a slight intensity loss in gradient echo (GRE) pulse sequence images [23]. The blood oxyhemoglobin in arterioles is diamagnetic and the blood deoxyhemoglobin in venules is paramagnetic. The BOLD technique takes an advantage of the fact that the neuronal activation induces change in the oxygenation level in venule blood [128]. The magnetic susceptibility of blood varies linearly with the blood oxygenation [183]. The susceptibility effect increases with magnetic field strengths. The BOLD signal is based on a microscopic susceptibility effect, so the signal-to-noise ratio (SNR) of the fMRI signal increases with higher magnetic field. Thus, higher fields are preferable for the detection of microscopic susceptibility effects.

The BOLD contrast reflects the hemodynamic response to neuronal activation. It is related to the blood flow and energy metabolism changes that accompany neural activity [23]. This relationship between local neural activity and subsequent changes in cerebral blood flow is called neurovascular coupling. The BOLD response is dependent on the dynamic properties of the vasculature that are altering the blood flow i.e. through physical dilation and constriction [23]. The positive BOLD responses correspond to a local overcompensation of blood volume for neural activation, which elevate the local oxygenation levels in venous blood [139]. A few candidate mechanisms for neurovascular coupling have been proposed: direct action of neuronally derived substances such as glutamate and nitric oxide on the vasculature, or cellular mediators including astrocytes, interneurons, and pericytes [66]. However, a consensus has yet to be reached in the field.

BOLD response can be illustrated as a time series of intensity values of pixels over fMRI experiment. Figure 3.2 shows the

BOLD response for a short stimulus. The response begins often with initial dip after which the MR signal intensity starts to increase typically within ~500 ms and it shows a peak at 3 s – 5 s after stimulus onset; this is known as the hemodynamic delay. After the peak activation, MR signal returns to the baseline, and often a post-stimulus undershoot of the signal is observed [109, 191].

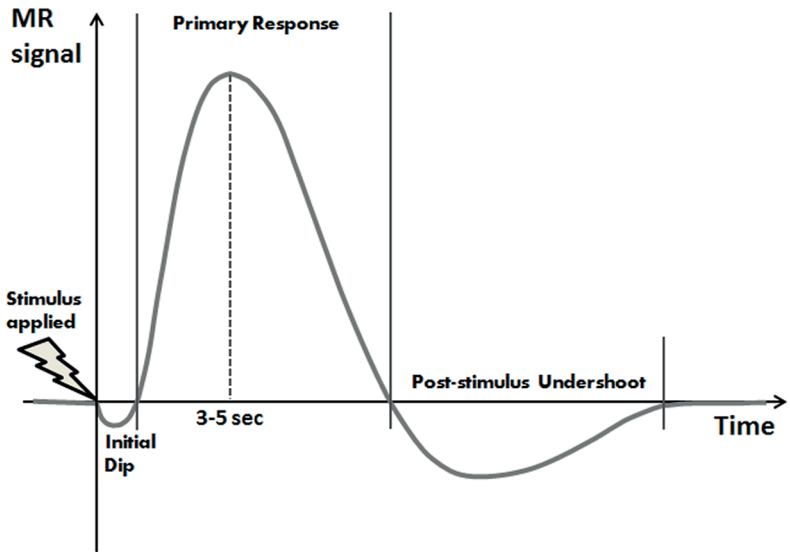

Figure 3.2: *The BOLD hemodynamic response. The intensity of a voxel varies just a few percent during hemodynamic response.*

The precise vascular and spatiotemporal dynamics of the actual cortical hemodynamic response to stimulation have been studied by means of optical imaging and two-photon microscopy [27, 67]. The neuronal activation seems to initiate dilatation of localized vascular volume. The increase in parenchymal concentration of total hemoglobin in capillaries occurs very early, prior to dilation of the pial arteries, and may be the underlying cause of the observations initially interpreted as the initial dip [27]. The post-stimulus undershoot of the BOLD response that is often observed is thought to be due to blood volume returning to baseline more slowly than the flow [22].

3.2.2 fMRI examination

There are several basic types of fMRI study paradigms available. A block design is the simplest and most frequently used experimental design of an fMRI study. During a block design fMRI experiment, the subject is performing a task in which there are periods of control task alternating with one or more activation tasks [101]. In a block design approach, the steady-state activation in one task is compared voxel-by-voxel to the steady-state activation in some other task or to the situation at rest [71]. The block design fMRI is sensitive at detecting the location of activation which explains why it is such a commonly used clinical application. One major clinical use is pre-surgical fMRI in patients with brain abnormalities [160] in order to localize the sensorimotor areas [13, 105, 184] or language lateralization [112, 159].

In an event-related fMRI paradigm, single trials of a particular stimulus are presented, and the responses are averaged time-locked to the stimulus presentation. This selective averaging approach directly provides a measure of the BOLD response on a voxel-by-voxel basis for the used stimulus type [23]. In other words, event-related designs are used in estimating the shape of the BOLD response during different trials, and also in comparing response parameters such as the amplitude or the timing between conditions. Event-related fMRI may be utilized for separating the elements of an experiment, to analysing cognitive processes associated with each element independently [70, 71]. For example, the brain regions contributing to individual processes within decision making, can be characterized by separating the components of different events from fMRI activation [72]. The event-related design is commonly used in research e.g. in psychiatric studies [116, 174], whereas it has been less extensively applied in diagnostics.

With the resting state fMRI, no repeated task or no task at all is performed during scanning. Functional connectivity between brain regions and local networks are explored by measuring the level of co-activation of resting-state fMRI time series between brain regions [173]. Resting-state fMRI makes it possible to

study the brain networks participating in long-lasting psychological or behavioural tasks, see e.g. [94].

A successful fMRI study depends on a good experimental design that distinguishes task-related signal from task-unrelated noise [4, 71]. The stimulation conditions and the timing of their presentation are crucial for evoking maximal changes in the cognitive processes of interest [71]. The experimental design affects all the phases of the fMRI experiment: hypothesis, data acquisition, pre-processing, and data analysis (see Figure 3.4).

If one wishes to conduct an fMRI scan, then fast T2* sensitive sequences are needed. Most BOLD studies use a GRE echo planar imaging (EPI) single-shot acquisition [125]. The EPI sequences are often employed for fMRI because of their short acquisition times and their high sensitivity to T2* changes. If one wishes to collect data from the entire brain, 30 or more slices are acquired during one repetition time (TR) depending on the slice thickness and orientation. In a typical fMRI experiment, TR varies between 1 s – 3 s. The spatial resolution which can be reached with EPI sequences in this short time window is a voxel size of 3 × 3 × 3 mm^3 for fMRI. In addition, the small signal changes caused by the BOLD effect (typically up to 5 % or 6 % @ 1.5T) make the relatively large voxel sizes reasonable in fMRI [47]. For signal enhancing, the sequence parameter time to echo (TE) should be approximately equal to local T2* relaxation time (40 ms – 60 ms), and the voxel dimensions should be optimized to discover the activated area [71]. The availability of a higher magnetic field in the fMRI scanner benefits the SNR of the fMRI. But also susceptibility effects increase with strength of magnetic field, so greater image artefacts are generated by susceptibility in higher magnetic fields [68].

3.2.3 fMRI analysis

After the fMRI data have been collected, the data need to be pre-processed prior to the statistical analysis. The fMRI scanner itself generates noise in the fMRI signal due thermal noise and system drift, which can be taken into account in the pre-processing phase. Physiological noise is induced from motion,

respiration, cardiac activity, and metabolic reactions [71]. Any slight movement of the subject's head will move parts of the subject's brain to another voxel locations, which is rather troublesome, especially if the motion is synchronized with the stimulus [53, 60]. The best way to minimize motion artefacts is to prevent motion by careful coaching of the subject and the application of head restraints. The manufacturers of fMRI scanners offer robust real-time calculation for statistics of block design experiments, which is a good technique also to monitor head motion. Motion effects can be corrected during fMRI scanning to a certain degree [156, 171, 181] or correction can be done off-line as a pre-processing step of data-analysis [30, 53]. The head motion can be estimated by matching the scans to a reference volume and the calculation of the transformation function at which the smallest value of the cost function is obtained. The original data are then resampled using the calculated realignment parameters [71].

The data from the entire brain contain 30 or more slices acquired during one TR. The time discrepancy between slices in scanning volume is corrected via temporal interpolation during pre-processing [71, 151].

The functional data are co-registered and visualized on high resolution structural images (Figure 3.3). If comparisons between several subjects are needed, then images of each subject's brain must be transformed to some common space with the same size and shape as all of the others being investigated. This spatial normalization mathematically stretches, squeezes, and warps the images of each brain into a common space, utilizing standard templates from the Montreal Neurological Institute [110] or Talairach space [163] as used as reference. Normalization with standard template should be undertaken with caution when comparisons are being made between different groups and one group has some kind of structural pathology [31]. To maximize the SNR, a spatial smoothing of functional images is commonly used with Gaussian filter with full width at half maximum (FWHM) of about two to three voxels [71].

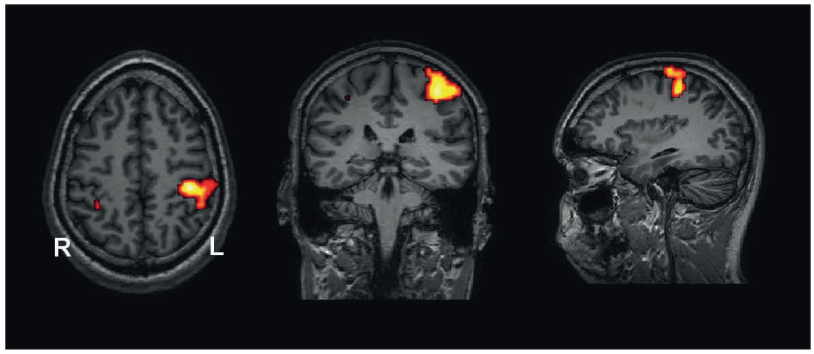

Figure 3.3: *fMRI activation of the right hand motor task. fMRI activation is shown on the T1-weighted image in transaxial (left), coronal (middle) and sagittal (right) view. Images are in radiological orientation.*

The basic analysis is to examine the time course in each voxel of the image, and identify those voxels in which the signal intensity changes synchronously with stimulus or task. The general linear model (GLM) [52] is a powerful and highly flexible technique for analysing fMRI data to estimate the strength and significance of activations in either block or event-related designs [23]. GLM treats the data as a linear summation of independent regressors (i.e. condition effects). In hypothesis testing, an experimenter creates a design matrix that contains regressors of interest as well as other sources of variability in the data. Statistical testing is used to determine how well a given regressor of interest predicts changes in signal intensity and whether some regressors lead to larger changes than others. The final result of the statistical analysis is a decision for each voxel, whether or not there is a significantly detectable activation [71].

In voxelwise statistics, a typical fMRI data analysis includes about 20 000 comparisons, which introduces the problem of multiple comparisons. The most common approach for the correction of multiple comparisons involves minimizing the number of false positive results, or controlling for familywise error (FWE) rate [117]. One standard strategy is to reduce the alpha value, so that voxels are less likely to pass the significance threshold due to chance. A rather stringent method for controlling FWE rate is to apply the Bonferroni correction [117] which adjusts the alpha value by dividing it by the number of

voxels presuming that time series in voxels are independent of each other. Functional neuroimaging data usually have some spatial correlation, thus may well be excessively conservative. Random field theory is used to estimate the number of independent statistical tests needed within analysis, based on the spatial correlation of the data [190]. An alternative approach controls for the false discovery rate, i.e. the proportion of false positives among rejected tests [58]. Furthermore, instead of whole brain examination, the interest may be focused on a specific area using anatomical region-of-interest (ROI) analysis. In a ROI analysis, the total number of statistical comparisons is greatly reduced and at the same time, the severity of correction for multiple tests can be reduced [135].

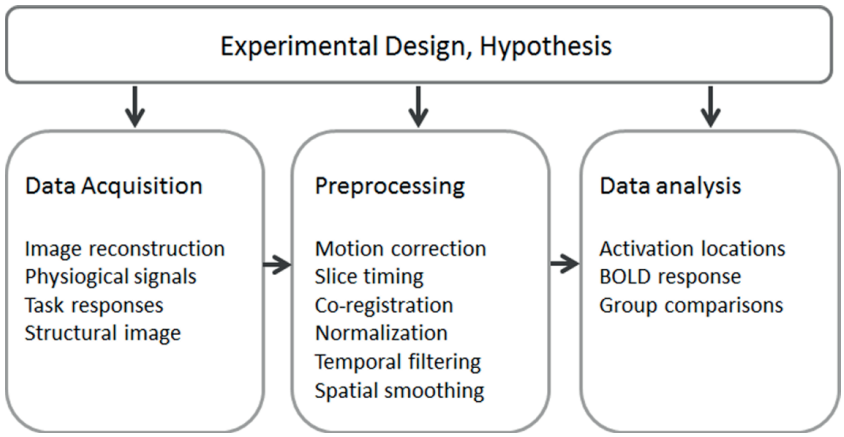

Figure 3.4: *Schematic illustration of an fMRI experiment.*

Figure 3.4 illustrates a schematic summary of an fMRI experiment. The result of fMRI analysis is usually a color-coded statistical parametric map of brain activation which can be displayed on top of an anatomical image. In the clinic, the diagnostic activation maps are presented on the subject's own high resolution MRI in individual space. Usually, a fast and easy analysis can be done with software implemented in an fMRI scanner.

3.3 TRANSCRANIAL MAGNETIC STIMULATION (TMS)

The first noninvasive stimulation of human brain was performed with electrical stimulation through the scalp by P.A. Merton and H.B. Morton in 1980 [113] but this application was too painful for clinical use. The TMS developed by A.T. Barker in 1985 [6] was a noninvasive and painless method to study cortical brain areas and the peripheral nervous system [6, 7, 141]. TMS applied on the primary motor area elicits muscle responses termed motor evoked potentials, which can be detected by electromyographic (EMG) recording. Single pulse TMS has been used to assess the cortical physiology and integrity of motor pathways [6].

3.3.1 Physiology of TMS responses

The time-varying magnetic field created by the current pulse in a coil gives rise to an induced electric field in brain tissue [7, 141]. The induced electric field in brain forces free charges into a coherent motion in both the intracellular and extracellular spaces. Cell membranes that interrupt this current flow become depolarized or hyperpolarized. If the depolarization is sufficient, an action potential may be initiated [142]. The activation of neurons depends on the strength of the applied electric field and its direction with respect to the neurons and their component parts. Straight, long axons are most easily stimulated at a point where the gradient of the electric field along the axon is at its strongest, whereas short axons are most easily stimulated at their ends. Curved axons are most easily stimulated at their bends, where the effective electric field gradient along the axon is the strongest [142]. The electric field in the cortex should be of the order of 100 V/m in order to elicit a cortical activation sufficiently strong to evoke hand muscle twitches [77] which can be detected as MEPs in the EMG recording. A voltage of 50 mV is usually defined as the minimum amplitude for MEP. When the hand motor area is stimulated, the latency of the MEP is about 20 ms (see MEP in right upper panel in Figure 3.6).

The cortical structures being activated by TMS have been identified by applying direct epidural recordings of corticospinal activity. The mapping has performed by stimulating the motor area with different TMS techniques and recording the responses from the epidural space of conscious patients with chronically implanted spinal electrodes [39-41]. When the induced current in the brain is directed perpendicular to the central sulcus and the stimulation intensity of TMS is the lowest possible to elicit the MEP, the response arises in pyramidal neurons in the cortical grey matter and it travels indirectly via trans-synaptic activation to the neurons of pyramidal tract [42]. The elicited response is known as an indirect wave, I-wave. When the induced current in brain is lateral-medial, first there can be a direct activation of the axons of fast pyramidal tract neurons just below the cortical grey matter. This response is called the direct wave, D-wave [42]. The response to TMS depends on the location and the direction of the induced current in the brain, the intensity of the stimulation, the shape of stimulation pulse, and the shape of the coil [39].

3.3.2 TMS examination

TMS is based on electromagnetic induction: a time-varying current in a primary circuit (TMS coil) induces an electric field and consequently a current flow (eddy current) in a secondary circuit (brain). During a TMS procedure, the coil is placed close to the head. The electric field induced in the brain by TMS depends on the shape of the coil, the location and orientation of the coil with respect to head, and the electrical conductivity structure of the scalp, skull, and brain [142]. Two main coil types are used in clinical work: a circular coil or a figure-of-eight coil. The region activated by the circular coil is roughly the area under the circumference of the coil [142]. The figure-of-eight coil is composed of two circular coils. By inducing two adjacent circular current distributions which sum together; the current densities in the tissue below the coil's centre are higher. Hence the field of the figure-of-eight coil is more concentrated and stronger than that obtained from a circular coil [142]. The figure-

of-eight coil is used for focal stimulation of cortex, e.g. it can be used for mapping of motor representation areas. Single-pulse TMS with circular coil is used to assess the pyramidal motor system and conduction times from cortex to muscle.

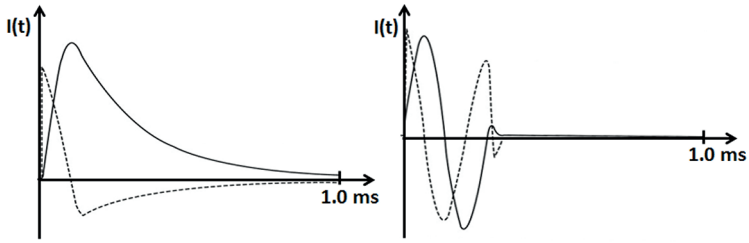

Figure 3.5: *Schematic illustrations of the monophasic (left) and biphasic (right) current pulses I(t) drawn with a solid line. Single-pulse devices have a current pulse duration about 600s for monophasic and 200 s – 300 s for biphasic pulse, the peak current is 2 kA – 8 kA [142]. The rate of current change dI(t)/dt is shown by a dashed line.*

The coil is connected to a pulse generator, which delivers electrical current to the coil. The current pulse generated in the coil is most commonly biphasic or monophasic (Figure 3.5), although also polyphasic pulses have been used [142]. In monophasic pulses, the coil current rises rapidly from zero to the peak value and returns slowly back. During the highest rate of change of the current in the coil, the induced electric field in brain is strongest and depolarization of cell membranes is possible [44, 142]. In biphasic pulses, the coil current rises rapidly from zero to its peak value and returns back, and then the current flows in the opposite direction in the coil. During both cycles of changing current, the voltage induced in the brain is highest at the beginning and around the midpoint of the pulse, but the fields are in opposite directions [44]. When stimulating the cortex or a nerve, biphasic stimuli are more effective and elicit compound muscle action potentials with lower thresholds and larger amplitudes than monophasic stimuli [118]. Monophasic stimuli are useful if one wishes to investigate excitation effects which are dependent on the current direction. The application of biphasic stimuli with their stronger

excitation effects might be advantageous when patients with high cortical thresholds need to be investigated [118].

When the head is modelled as a sphere, the induced electric field is always parallel to the nearest sphere surface and there is no radial electric field [142]. The strength of the magnetic field decreases rapidly as a function of distance from the coil [44]. With circular or figure-of-eight coils, it is not possible to stimulate deep brain structures without stronger stimulation of the more superficial cortex [77].

Traditionally a TMS pulse with the circular coil is targeted to hand motor area by placing the coil centre on the vertex of the head. In this setup, the edge of the coil lies over the motor hand-arm area and crosses the precentral gyrus perpendicularly [142]. The figure-of-eight coil tends to be focused in the cortical site of interest by determining anatomical landmarks or according to the International 10–20 EEG electrode positioning system [82]. However, it is possible to improve the accuracy of the TMS by applying navigation. In nTMS, the stimulating coil can be positioned stereotactically above the target location on the basis of MR images [142]. The nTMS system provides on-line navigation with the option to repeat the TMS pulses to a certain anatomical structure by storing the information of the coil position, tilting, and orientation with respect to the subject's head. By integrating the stimulus-induced electric field distribution calculations [143] to the navigation system, the visualization of the induced electric field can be used online during stimulation and the sites of stimulations can be saved for a later examination.

3.3.3 TMS analysis

TMS offers high sensitivity in detecting abnormalities of corticospinal pathways and it is used in diagnosing and monitoring neurological disorders with upper motoneuron involvement [145]. A variety of MEP parameters can be studied: the latency and the size of MEP (amplitude, duration, area) and stimulation intensity threshold for MEPs [195]. The most widely used parameter is the latency of MEP. Latency is influenced by

the subject's height, limb length, and possible abnormalities in peripheral nerve conduction [64]. The reference values for latencies as a function of length and age are recommended for good clinical practice. The minimum stimulation intensity sufficient to produce a MEP in predefined muscle at least 50 % of trials is called the motor threshold [140]. The MT reflects the excitability which arises from the excitability of individual neurons and their local density [61].

MEP mapping, mapping the motor area by moving the coil over the surface of the scalp and recording MEPs from different muscles, is a fairly straightforward clinical application [61] (Figure 3.6). MEP mapping with nTMS has proven to be reliable for pre-surgical mapping of primary motor areas in tumour patients [51, 88, 132, 133] when compared to direct cortex stimulation during brain surgery.

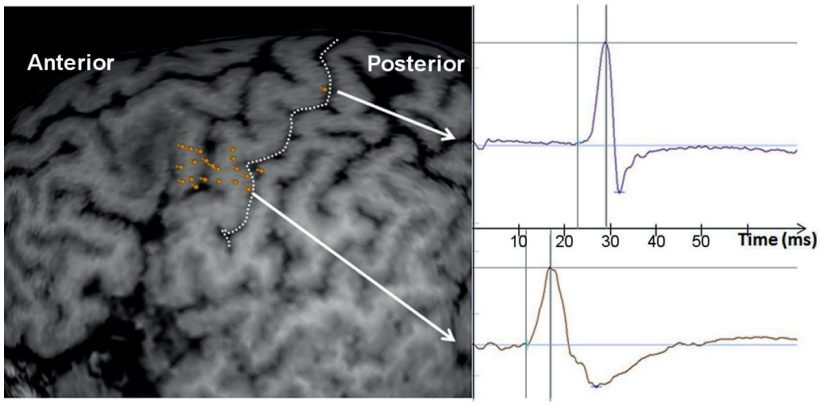

Figure 3.6: *A navigated TMS study on the left hemisphere. Stimulation locations on left hemisphere motor representation areas of thenar muscle (medial location) and facial muscles (lateral locations) are shown in the left panel. Elicited MEPs from thenar muscle (upper MEP with latency of 23 ms) and facial muscle (lower MEP with latency of 11 ms) are shown in the right panel. The peak-to-peak amplitude of 50 mV is usually defined as minimum amplitude for MEP. The central sulcus is enhanced with the white dotted line.*

rTMS involves stimulation with a train of magnetic pulses at frequencies between 1 Hz and 50 Hz or even higher. rTMS can produce powerful effects that outlast the period of stimulation:

inhibition with a stimulation at about 1 Hz and excitation with a stimulation at 5 Hz and higher [61]. The effect of rTMS has been utilized in therapy, e.g. applied on the dorsolateral prefrontal cortex to treat major depression (see review [57]) or on the M1 area to treat chronic pain (see review [55]). Furthermore, rTMS-induced effects have been used as a tool to disrupt temporarily cortical activity occurring locally under the coil or indirectly for remote cortical areas [195]. rTMS has been applied to identify the speech area without navigation [5, 38, 45, 50, 158]. One recent study has shown that language function mapping with navigated rTMS correlated well with intraoperative DCS [131].

4 Aims of the present study

The goal of this PhD study was to investigate the feasibility of clinical neuroimaging tools for studying the functions of the cerebral areas which participate in the execution of motor tasks e.g. motor action and speech. The specific aims were:

1. To use clinical neuroimaging tools, SPET, fMRI, and TMS to detect changes in the functionality of the motor area induced by CIMT, a rehabilitation program for chronic stroke patients. (Studies **I** and **II)**

2. To utilize fMRI to detect altered motor activation related to impaired motor performance in patients with Unverricht-Lundborg disease. (Study **III**)

3. To combine rTMS and fMRI to localize the functional areas involved with motor control and production of speech. (Study **IV**)

5 Materials and methods

This thesis consists of four studies. The longitudinal studies (Studies **I** and **II**) evaluated the capability of clinical methods to detect changes in neuroplasticity in chronic stroke patients who had been subjected to CIMT rehabilitation. In Study **III,** fMRI was used to detect the possible alterations in cortical activation related to motor performance in EPM1 patients in comparison with healthy volunteers. In Study **IV**, a combination of rTMS and fMRI was used to clarify the localization of the functional areas involved with motor control and production of speech.

5.1 SUBJECTS

Detailed subject demographics are shown in Table 5.1. Written informed consent was obtained from all subjects in accordance with the Code of Ethics of the World Medical Association (Declaration of Helsinki, http://www.wma.net/en/30publications /10policies/b3/), and the protocols were approved by the ethical committee of the Northern Savo Hospital District.

Table 5.1: *Subject demographics, number of females and males, and the age (years) as the group mean and standard deviation.*

Study	Subjects	Number of females /males	Age (years)
I	stroke patients	4 / 8	47.7 ± 10.3
II	stroke patients	4 / 7	46.9 ± 10.4
III	EPM1 patients	8 / 7	32.2 ± 10.9
	volunteers	8 / 7	32.7 ± 11.0
IV	volunteers	5 / 4	38.3 ± 8.6

In Studies **I** and **II**, 13 chronic stroke patients were enrolled in a two-week CIMT program. The entry criteria for CIMT were: (1) ≥ 6 months from the first ischemic stroke, (2) a minimum

voluntary control of 10 degrees for the wrist and fingers [115], (3) no severe communication problems, and (4) no other acute diseases. Five subjects had right and eight had left hemiparesis. The characteristics of the individual patient are shown in Table 5.2. The subjects were examined on two different days, one before and the other after the two-week therapy. During the day, all subjects first underwent the TMS examination, then SPET, and finally fMRI.

Table 5.2: *Stroke patient demographics, including age (years), the time since stroke onset (months) and location and extent (cm) of major lesion in MR images.*

Patient characteristics			**Details of maximum lesion in MRI**				
Sex	**Age (yrs)**	**Time (mths)**	**Side**	**Deep**	**Cortical**	**Size (cm)**	**Studies**
M	53	37	R	Yes	No	3.0	II
F	46	12	L	Yes	No	1.2	I, II
M	52	16	R	Yes	No	1.0	I, II
F	64	30	L	Yes	Yes, M1	7.0	I, II
M	54	18	NA	NA	NA	NA	I
M	53	24	R	No	Yes, M1	11.5	I, II
F	30	72	L	No	Yes, M1	9.0	I, II
F	48	12	R	No	Yes, M1	7.0	I, II
M	41	18	R	Yes	No	2.0	I, II
M	32	132	R	Yes	Yes	7.0	I, II
M	40	43	R	No	Yes, M1	17.0	I, II
M	55	24	L	Yes	No	3.5	I
M	57	7	L	No	Yes, M1	5.0	I, II

F, female; M, male; NA, not available; M1, primary motor area; Side, lesion hemisphere; Size, maximum diameter of major lesion in transaxial MRI

In Study **III**, 16 patients participating in the large EPM1 cohort study were recruited to participate to additional motor fMRI task. The mean of the duration of disease was 22.1 years with a range from 4 years to 36 years. All patients were treated with antiepileptic medication at individually titrated combinations and dosages. The severity of symptoms of the EPM1 patients was characterized using a myoclonus action score (AM) from a unified myoclonus rating scale [54] in which

the maximum score is 160, with higher scores indicating more severe symptoms. The mean of the AM was 49.9 points with a range from 8 to 90 points. One subject was not able to perform the motor fMRI task because of severe myoclonus, and had to be excluded from the study. A total of 15 healthy volunteers matched for age and gender were recruited as control subjects and performed the same motor fMRI task.

In Study **IV**, in the rTMS study, there were 10 subjects who volunteered to take part; these were part of a previous group of 20 healthy adults who had participated in a language fMRI study one year earlier [119]. One participant had to be excluded from the study because the resting motor threshold of her abductor pollicis brevis (APB) muscle was too high to be determined with used system. One participant was left-handed and one was ambidextrous, according to the 20-item modified Edinburgh Handedness Inventory [124].

5.2 SINGLE PHOTON EMISSION TOMOGRAPHY (STUDY I)

5.2.1 Cerebral perfusion SPET examination

In the SPET imaging a dose of 550 MBq of ^{99m}Tc-ECD (Neurolite, Dupont Pharma/Durham APS, Kastrup, Denmark) was intravenously injected into the subject's right antecubital vein in a dim and quiet room. The SPET scan was carried out 45 to 60 minutes later with a three-head Siemens MultiSPET 3 gamma camera (Siemens Medical systems Inc., Hoffman Estates, IL, USA) equipped with fan beam collimators [91]. The radius of the rotation was 13.8 cm; with a total of 5 – 7 million counts; an angular step of 3° over 360°; the matrix size 128 x 128; 40 projections/camera head and each 35 s; the total imaging time was 25 minutes.

Three millimeter thick transaxial slices were reconstructed using a 6th order Butterworth filter with a cut-off frequency of 0.5 cm^{-1}. The Chang attenuation correction [26, 28, 136] with a uniform attenuation coefficient of 0.12 cm^{-1} was applied. The imaging resolution was 7 mm – 8 mm. The slices were

consecutively summarized into a total slice thickness of 6 mm for further analysis.

5.2.2 Cerebral perfusion SPET analysis

First, all transaxial slices of those patients whose lesion was in the left hemisphere, were mirrored. After mirroring, all lesions were located in the affected "right" hemisphere. The "left" hemisphere was the non-affected hemisphere. SPET images from both examinations were realigned into the same position. The individual SPET images were normalized into the same stereotactic space using bilinear interpolation, and then smoothed by a Gaussian kernel with 11 mm FWHM (SPM99, Wellcome Department of Imaging Neurosciences, Institute of Neurology, UCL, London, UK; and MATLAB, The Mathworks Inc., Natick, MA, USA). The resolution in the statistical parametric mapping (SPM) analysis was 2 x 2 x 2 mm^3. The statistical group analysis was carried out by the paired t-test comparing the perfusion before the therapy to the perfusion after the therapy. Proportional scaling was performed for the t-test by scaling the global mean to the value of 50 ml/dl/min. Threshold masking was also proportional, i.e. 80% of the mean global value, to ensure that only grey-matter voxels were included in the analysis. The global value was calculated as a mean voxel value: first the mean of overall voxels in the image was calculated, voxels which did not reach a threshold of the overall mean divided by 8 were masked out (i.e. those which are extra-cranial), followed by a second computation of the mean of the remaining voxels. Clusters with p-value ≤ 0.001 and size > 20 voxels (160 mm^3) were considered as significant.

5.3 FUNCTIONAL MAGNETIC RESONANCE IMAGING (STUDIES II, III, AND IV)

5.3.1 fMRI and MRI examinations

Structural three dimensional T1-weighted images were obtained for anatomical reference using a magnetization-prepared rapid

acquisition gradient-echo (MPRAGE) sequence with an isotropic resolution of 1 mm^3. Table 5.3 shows the scanners, coils, and details of the sequences used in the different studies. In Studies **I** and **II,** which was intended to clarify the details of the lesions, conventional T1-, T2-, proton density-weighted images and fluid attenuated inversion recovery images were obtained. In order to exclude any acute ischemic lesion, diffusion weighted imaging was also performed. All MR images were examined visually by an experienced neuroradiologist.

Table 5.3: *MRI scanners, coils and repetition time TR (ms), time to echo TE (ms) and inversion time TI (ms) for T1-weighted MPRAGE sequences*

Study	Scanner	coil	TR (ms)	TE (ms)	TI (ms)
II	Siemens Vision 1.5T	head coil	9.7	4.0	20
III	Siemens Avanto 1.5T	tx/rx coil	1980	3.09	1100
IV	Siemens Avanto 1.5T	8-channel head coil	1980	3.09	1100

tx/rx coil, transmit/receive head coil

BOLD sensitive fMRIs were obtained using an EPI sequence, with the parameters shown in Table 5.4. Block design fMRI task paradigms were used in all studies. In Studies **II** and **III**, a motor task paradigm was used in which the paradigm consisted of blocks of repetitive movements of all fingers (flexion/extension) alternated with rest periods. The task was practiced before scanning and the performance was visually monitored. In Study **II,** movements were paced by visual guidance at 0.5 Hz, the task consisted of blocks of either left or right hand voluntary movements or rest. In Study **III**, the participants performed self-paced repetitive movements with the right hand, the starts and stops of the movement blocks were instructed via auditory commands. In Study **IV**, a word generation task was used. The paradigm consisted of four blocks of the active condition in which the task was to covertly generate different words starting with the visually given alternating letter (one letter per block). In the control condition, subjects were shown a fixation cross and were instructed to stop generating words and instead to perform a simple self-paced

finger tapping task alternating with the right and left index fingers. The task paradigms are summarized in Table 5.5.

Table 5.4: *Parameters for EPI sequences, resolution (mm^3), number and orientation of slices, repetition time TR (ms), and time to echo TE (ms) and flip angle (°)*

Study	Resolution (mm^3)	Slices	Plane	TR (ms)	TE (ms)	Flip angle(°)
II	4 x 4 x 4	34	in AC-PC	4000	72	90
III	3 x 3 x 3	36	in AC-PC	3540	50	90
IV	3 x 3 x 3	36	in AC-PC	3100	50	90

AC-PC, plane which runs through the anterior commissure and posterior commissure and is perpendicular to the parasagittal plane

Table 5.5: *Structures of the task paradigms*

Study	Task [Reference task]	Guidance	A/B	Length of block
II	flexion-extension, all fingers, 0.5 Hz, left/right hand [rest]	visual	6/6	12 scans
III	flexion/extension, all fingers right hand [rest]	auditory	3/3	10 scans
IV	covert word generation [finger tapping]	visual	4/5	10 scans

A/B, Number of blocks of activation and baseline, in Study II both the left and right hands performed the activation task separately in six blocks.

5.3.2 fMRI analysis

Functional MRI data was analysed with the SPM5 (Study **II** and **IV**) and SPM8 (Study **III**) software packages (the Wellcome Trust Center for Neuroimaging, UCL, London, UK, www.fil.ion.ucl.ac.uk/spm/) running under Matlab R2007a (The Mathworks Inc., Natick, MA, USA). Pre-processing of the images started with motion correction, correction of the acquisition time difference between slices, and co-registration to individual anatomic T1-weighted images. In Studies **II** and **III**, in the group analysis the images were normalized into stereotactic space (voxel size of 2 x 2 x 2 mm^3), whereas in Study **IV**, the images were maintained in individual space for rTMS comparison and converted in MNI space for laterality index (LI) calculation. Finally, the images were spatially smoothed with a Gaussian kernel of FWHM of twice the original pixel size.

Statistical analysis was performed on a voxel-by-voxel basis using the GLM [190], comparing the active condition and the control condition with a T-test.

The ROI based analyses were performed to focus on the activations of motor related areas or language areas, or to analyse the lateralization of activations (Table 5.6). In Study **II**, the ROI approach was used to quantify fMRI activity in sensorimotor and premotor cortical areas. In Study **III**, fMRI analysis was focused on the left M1, left S1 and bilateral SMA areas. In addition to the M1 ROI, the hand knob [193] was outlined as a separate ROI. All individual M1 ROIs were further combined together to form a mask ROI which was used in the group analysis. In Study **IV** for the LI calculation the language ROIs were defined as a combination of Broca area, Wernicke area, Heschl gyrus and the hippocampus, on the left and the right hemisphere separately.

Table 5.6: *Regions of interest ROI used in the studies*

Study	Definition of the ROI	Origin
II	Sensorimotor (SM1) Premotor (PMA) Affected / non-affected hemisphere	Individual WFU PickAtlas
III	Left primary motor (M1) Left primary sensor (S1) Left hand knob Bilateral supplementary (SMA)	Individual Individual Individual Individual
IV	Language ROI: Broca area, Wernicke area, Heschl gyrus and the hippocampus. Left / Right hemisphere	WFU PickAtlas

WFU PickAtlas: http://fmri.wfubmc.edu/software/pickatlas

Hemispheric dominance was assessed via the laterality index of activations. LIs were calculated for motor activation in Study **II** to clarify if activation was contralateral, ipsilateral or bilateral. Hemispheric dominance of language function was defined by LI in Study **IV**. The sum of positive T-values across all voxels within the ROIs separately for the contralateral (C) and ipsilateral (I) hemispheres in case of motor activation, and for

the left (C) and right (I) hemispheres in case of language activation were calculated. The LI was calculated LI = [(C-I)/(C+I)].

In Study **II**, the magnitude of the fMRI activity was defined as the percent (%) signal change between the mean intensity of the motor and rest conditions across all voxels in ROIs. The contrasts between pre- and post-training activations were calculated, and the volumes of increased or decreased activation were defined separately for paretic and non-paretic hand movements individually as the number of significant voxels ($p < 0.05$, FWE-corrected, clusters of ≥4 voxels) in ROIs. These quantitative parameters of fMRI were correlated with lesion parameters, clinical parameters and TMS results.

In Study **III**, the result of group comparison was focused in a ROI which was combination of all individual M1 ROIs. Additionally, quantitative fMRI parameters were compared between groups: From the individual T-maps, the number of voxels with positive T-values, the mean and maximum of positive T-values surviving the familywise error corrected threshold of $p < 0.05$ in each ROI were evaluated. These fMRI parameters were also correlated with the myoclonus via MA and disease duration in EPM1 group and with age in both EPM1 and control groups.

In Study **IV**, the active word generation condition and the control condition were compared. The T-maps in individual space with threshold of uncorrected p-value less than 0.001 were generated for the TMS comparison. Table 5.7 summarizes the quantitative fMRI parameters.

Table 5.7: Calculated quantitative parameters from ROIs

Study	ROI	Parameters	Test
II	SM1, PMA	laterality index, percent signal change, number of voxels in pre-post contrast (increased/ decreased activation)	Comparison Before-After Correlation to TMS
III	M1, S1, SMA, hand knob	number of activated voxels, maximum of T-values, mean of T-values	Comparison EPM1-Controls Correlations in EPM1
IV	language area	laterality index	

SM1, primary sensorimotor area; PMA, premotor area; M1, primary motor area; S1, primary somatosensory area; SMA, supplementary motor area

5.4 TRANSCRANIAL MAGNETIC STIMULATION (STUDIES II AND IV)

5.4.1 TMS examination

In Study **II**, a non-navigated TMS with fixed stimulation parameters was used to study a modulation in cortical hand motor area excitability induced by CIMT rehabilitation. The magnetic stimulator MES-10 (Cadwell Laboratories Inc., Kennewick, WA, USA) with a circular 9 cm diameter coil was used to achieve the TMS. First the non-affected hemisphere and then the affected hemisphere were stimulated. The coil was moved systematically over the hemisphere, and five stimulation locations were used: C4/C3, FC4/FC3, C6/C5, CP4/CP3 and C2/C1 according to the International 10–20 System routinely used for EEG recording. The stimulation intensity was 90 % of maximum stimulator output in first phase. Then the location which gave the maximum muscle response was stimulated again twice with 60 % intensity during voluntary hand muscle contraction. Four channels of surface EMG (filter bandpass: 10 Hz – 5 kHz) were recorded with standard EMG equipment (Nicolet Viking IV, Dantec, WI, USA) from muscles abductor pollicis brevis and abductor digiti minimi bilaterally.

In Study **IV**, navigated rTMS with short bursts was used to map the speech areas on both hemispheres by inducing speech disruption during number recitation tasks in healthy volunteers. The Magstim Rapid stimulator (Magstim Company Ltd, Whitland, Wales, UK) and figure-of-eight coil (Double 70mm, PN9925) were connected to a stereotactic on-line Navigated Brain Stimulation system (eXimia software version 3.1., Nexstim Plc, Helsinki, Finland) to enable visualization of the stimulation coil in relation to the cortical anatomy and storing the stimulation location. Individual three dimensional T1-weighted MRIs were used for navigation. Figure 5.1 illustrates the navigated rTMS examination. The resting MT of the right APB muscle was determined using the Rossini-Rothwell method on the left hemisphere [140, 144]. The MT was used to adjust the stimulation intensity during examination.

Mapping of the motor speech area was performed during the overt number reciting task, which was chosen as an easy, fluently speech-producing task. Participants were instructed to continuously recite numbers aloud and to try to continue reciting even if their speech was disturbed. Stimulation bursts were delivered from one to three seconds after the voluntary recitation of numbers had started. The mapping was initiated by focusing the nTMS at the posterior frontal lobe areas of the left hemisphere. The stimulus intensity was initially 120 % MT, and it was elevated in 10 % MT increments to a maximum of 150 % MT, or until subjective speech disruption was reported or observed. The stimulation area was extended concentrically until there was no disruption in speech. Bursts of stimuli were applied with spacings of 5 mm – 10 mm. The corresponding posterior frontal lobe area of the right hemisphere was stimulated similarly.

All stimulation sessions were also recorded for offline analysis (video and audio), and the recordings were segmented to samples of trials for blinded reviewer evaluation.

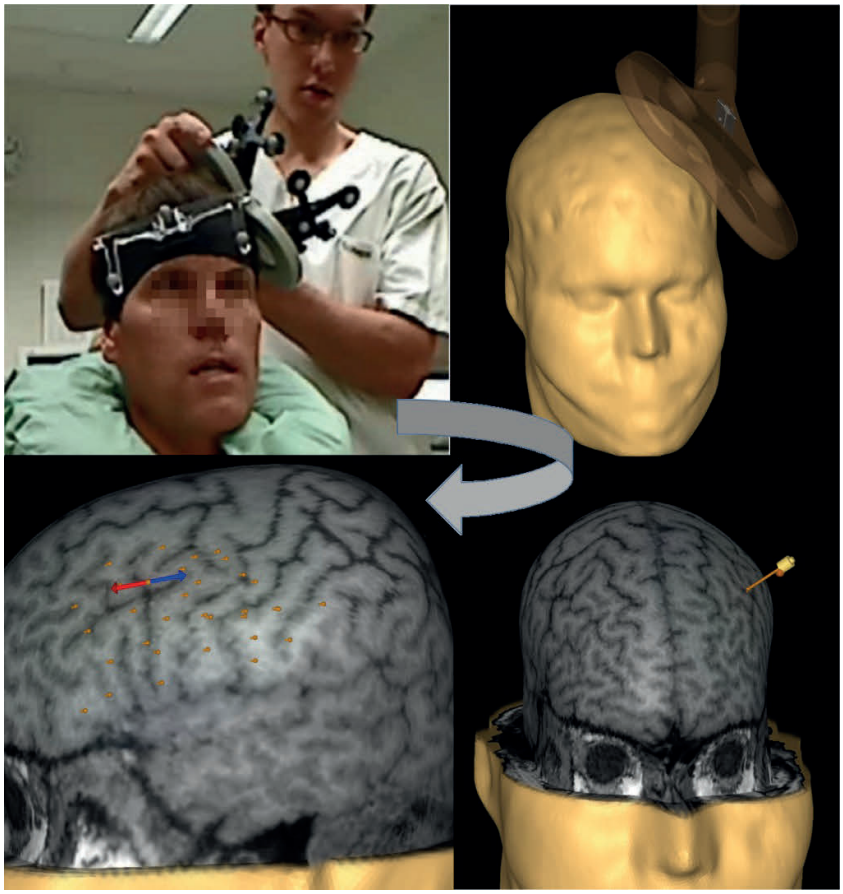

Figure 5.1: *Navigated repetitive magnetic stimulation, rTMS with short bursts was used to map the speech areas. The upper left panel shows the situation of stimulation, the subject and the stimulation coil are equipped with reflectors for the optical tracing and navigation. The upper right panel shows the coil location on the visualized head in eXimia software (Nexstim Plc). The lower right panel shows the coil location with a yellow cylinder on the visualized brain surface based on MRIs. The lower left panel shows all stimulation locations, and the red-blue array presents the direction of TMS induced current of the used coil location.*

5.4.2 TMS analysis

The onset latencies and the baseline-to-peak amplitudes of the MEPs after stimulation were measured in Study **II**.

The analysis of speech disruptions was triphasic in Study **IV** (Table 5.8). The first phase was an online evaluation. Each participant assessed his/her subjective experience after

stimulation burst. They judged whether their speech had been disrupted: (1) "definitely", (2) "possibly" or (3) "definitely not", they described also how the speech was disrupted. The level of pain was also assessed by a numeric rating scale (0 means no pain, 10 means the worst imaginable pain) and furthermore the appearance of distracting muscle contractions was enquired.

The second phase was the review of the video samples. Two experienced clinicians analysed the video samples separately and blinded to the location of stimuli. Both reviewers graded each trial using three clinically relevant classifications: (Class 1) words are unrecognizable, or there is a speech arrest or aphasia (speech disruptions, as in the Wada test [169, 180]); (Class 2) pronunciation is significantly disrupted or imprecise, but words are recognizable; or (Class 3) there is no detectable disruption.

The third phase was the categorizing the effects of stimuli in different locations further using the evaluations of the two reviewers when the volunteer experienced definitive speech disruption subjectively. Category 1: both reviewers agreed with the grade that the words were unrecognizable or there was arrest or aphasia (Class 1). Category 2: one reviewer evaluated significant disruption in speech or in pronunciation (Class 1 or 2) and the other reviewer evaluated significant disruption in pronunciation (Class 2). Category 3: only one reviewer judged that at least a significant disruption in pronunciation had occurred (Class 1 or 2). Category 4: no objective finding judged by the reviewers.

The nTMS sessions and T-value maps of fMRI were imported to eXimia software version 3.2 which allowed visualization of both methods simultaneously. The rTMS locations were presented over each subject's T-value map and examined visually.

Table 5.8: Categorization of the rTMS effects for speech task

Subjective evaluation			
Yes:	Speech was definitely disrupted		
No:	Speech was possibly or definitely not disrupted		
Reviewer's evaluation			
Class 1:	Words are unrecognizable, or there is a speech arrest or aphasia		
Class 2:	Pronunciation is disrupted or imprecise, but words are recognizable		
Class 3:	No detectable disruption		
Category of the effect	**Subjective**	**Reviewer 1**	**Reviewer 2**
Category 1	Yes	1	1
Category 2	Yes	1 or 2	2
Category 3	Yes	1 or 2	3
Category 4	Yes	3	3

5.5 STATISTICAL TESTS

Statistical tests for different parameters were performed with SPSS software (Versions 9.0, 17.0 and 19.0, IBM Corporation, Somers, NY, USA). Non-parametric tests were used for small and not normally distributed material: Mann-Whitney U for independent group tests, Wilcoxon test for related group tests, Kruskal-Wallis test for independent group tests, and Spearman's rho correlation coefficients for relationships between different variables. The level of significance was set at $p < 0.05$.

5.6 ADDITIONAL METHODS

5.6.1 Constraint-induced movement therapy (CIMT) (Studies I and II)

In CIMT therapy, a light-weight loose cast was fitted on patient's non-affected hand and wrist to mechanically limit movement during exercises and daily activities. The patients were encouraged to wear the cast for about 10 hours/day. The cast included a body temperature-activated clock. The increasingly challenging individual exercises for the affected

hand were timed to keep the motivation level high. The duration of the CIMT rehabilitation program was two weeks (5 days a week, 6 hours/day) [115, 168].

5.6.2 Structured motor function test (Studies I and II)

A structured motor function test, i.e. the Wolf motor function test (WMFT) [187], was performed to assess the motor behaviour of the affected arm and hand. This test has 16 motor tasks, such as dragging of a 500 g weight a designated distance on the table or picking up a pencil from a predetermined place. Each task is timed and scored in terms of both functionality (score range 0 – 5) and quality (score range 0 – 5) of movement. The maximum score of 80 points in functionality and 80 points in quality of movement is easily attainable with a healthy hand and arm.

6 Results

6.1 FUNCTIONAL CHANGES IN MOTOR RELATED CORTICAL AREAS INDUCED BY CIMT IN STROKE PATIENTS (STUDIES I AND II)

6.1.1 Motor functions

The accomplished hours of exercise were 53.4h ± 1.8 h expressed as mean ± SD, with a mean duration of the cast wear of 80.0 h ± 14.2 h. Two weeks of CIMT rehabilitation resulted in an improvement in the voluntary hand motor control in the paretic hand. The mean total time obtained in the WFMT decreased significantly after therapy ($p = 0.035$) and the mean functionality and quality scores improved significantly ($p = 0.002$ and $p = 0.002$, respectively).

6.1.2 Cerebral perfusion SPET results

Cerebral perfusion at rest changed in both hemispheres after the two-week long rehabilitation therapy when compared with the pre-therapy values. The motor specific areas with the perfusion increase were in the precentral gyrus in the affected hemisphere and in the superior frontal gyrus in the non-affected hemisphere. Several other areas were identified as exhibiting changed cerebral perfusion, see Table 6.1 and Figure 6.1. The perfusion was increased in the cingulate gyrus in the non-affected hemisphere and in the superior frontal gyrus in the affected hemisphere. There were also some areas which displayed a decrease in perfusion i.e. the lingual gyrus in the affected hemisphere and two areas in the middle frontal gyrus in the non-affected frontal cortex. In addition, an area in the fusiform gyrus and an area in the inferior temporal gyrus showed evidence of decreased perfusion.

Table 6.1: *The effect of CIMT in cerebral perfusion measured by SPET. Areas with statistically significant change in perfusion: Corresponding Brodmann areas BA, Talairach coordinates X,Y,Z, and the size of cerebral area in voxels are shown.*

		Talairach			
Area, Brodmann area	**Change**	**X**	**Y**	**Z**	**Size (voxels)**
Motor and Premotor areas					
Superior frontal gyrus, BA6	+	-8	18	56	65
Precentral gyrus, BA6	+	22	-18	76	67
Other					
Superior frontal gyrus, BA10	+	8	60	-5	54
Medial frontal gyrus, BA10	-	-38	40	20	24
Medial frontal gyrus, BA8	-	-50	12	46	27
Fusiform gyrus, BA20	-	-42	-13	-21	145
Cingulate gyrus, BA31	+	-10	-35	37	65
Inferior temporal gyrus, BA37	-	-50	-45	-7	111
Lingual gyrus, BA18	-	10	-75	9	187

+ denotes increased cerebral perfusion; - denotes decreased cerebral perfusion. A negative x-coordinate denotes the non-affected hemisphere, and a positive x-coordinate denotes the affected hemisphere.

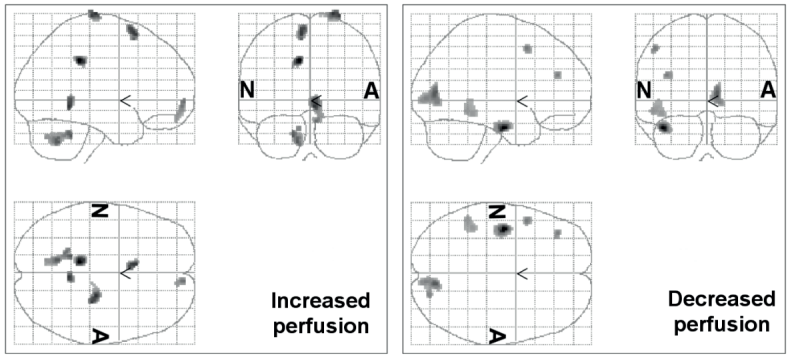

Figure 6.1: *The effect of CIMT in cerebral perfusion measured by SPET. Areas with a change in cerebral perfusion: areas of increased perfusion in the left panel and areas of decreased perfusion in the right panel (SPM99, Wellcome Department of Imaging Neurosciences, Institute of Neurology, UCL, London, UK). A denotes the affected hemisphere, and N denotes the non-affected hemisphere.*

6.1.3 fMRI results

Ten patients performed the fMRI task of repetitive flexion and extension of all fingers with the paretic and non-paretic hand separately. The dimensions of the movements were not measured, but everyone was encouraged to do his/her best with the paretic hand movements. Three patients had unintentional feet movements during the fMRI task before CIMT, but not after CIMT. One patient performed repetitive abduction of the little finger (because of limited hand function) and exhibited minor mirror movements during the first session.

The activation laterality on sensorimotor ROI was significantly different depending on which hand was performing the task: The movement of the paretic hand induced less contralateral sensorimotor activity than the movement of the non-paretic hand, both before and after CIMT. The laterality of premotor activation did not reach a statistically significant difference before CIMT between tasks of paretic and non-paretic hand, but after CIMT, the LI was significantly lower for the paretic in comparison with the non-paretic hand (LI = -0.027 ± 0.024 for paretic hand task vs. LI = 0.221 ± 0.348 for non-paretic hand task ($p = 0.041$)).

The percent signal change in both ipsilateral ROIs were higher for the paretic hand task than for the corresponding task with the non-paretic hand at both time points (PMA: before CIMT, $p = 0.010$ and after CIMT, $p = 0.003$; SM: $p = 0.007$, $p = 0.003$, correspondingly). The correlations between the magnitude of fMRI signal change in different ROIs and clinical parameters are presented in Table 6.2.

Changes were found in fMRI activation due to CIMT; the volumes of changed activation in different ROIs were parallel in both the paretic and non-paretic hand tasks. However, the volume of decreased activation in the contralateral pre-motor area was significantly higher ($p = 0.012$) in the paretic hand task (volume = 112 ± 138 voxels) than when the task was performed with the non-paretic (volume = 23 ± 51 voxels). The correlations

between the volume of changed fMRI activation in different ROIs and clinical parameters are presented in Table 6.2.

Table 6.2: *The correlation coefficients between fMRI and clinical parameters, the p-value of correlation is shown in parentheses.*

Clinical parameter	The fMRI ROI	Paretic hand task	Non-paretic hand task
The magnitude of fMRI signal change			
	Before CIMT		
Lesion diameter	non-affected PMA	-.679 (.022)	n.s.
Lesion diameter	affected SM1	-.630 (.038)	n.s.
Time from stroke	affected PMA	-.721 (.012)	-.656 (.028)
WMFT time, pre	affected PMA	-.670 (.024)	n.s.
WMFT time, pre	affected SM1	-.606 (.048)	n.s.
	After CIMT		
Lesion diameter	affected PMA	n.s.	-.651 (.030)
Lesion diameter	affected SM1	-.795 (.003)	-.734 (.010)
Time from stroke	non-affected PMA	-.788 (.004)	n.s.
Cast wearing time	affected SM1	.729 (.011)	n.s.
Extent of CIMT induced increase in fMRI activation			
WMFT time, pre	affected SM1	.670 (.024)	n.s.
WMFT score, pre	affected SM1	-.731 (.011)	n.s.
WMFT time, change	affected SM1	-.606 (.048)	n.s.
WMFT score, change	affected SM1	.661 (.027)	n.s.

Pre: before CIMT, SM1: primary sensorimotor area, PMA: premotor area, WMFT: Wolf Motor Function Test, n.s.: not significant

The individual lesions as well as the increases in fMRI activation associated with the therapy in three representative cases are shown in Figure 6.2. An evident activation increase occurred in the SM1 area of the affected hemisphere (circled in green) in patients whose paretic hand motor function improved markedly in comparison to the baseline. The depth of the lesion location was also related to the shift in the activation pattern: patients with subcortical lesions (n = 4) had greater activation increases during the non-affected hand task in SM1 areas bilaterally than occurred in the patients with cortical lesions (n = 7) ($p < 0.012$). However, the specific location of the lesion exerted no systematic effect on fMRI findings.

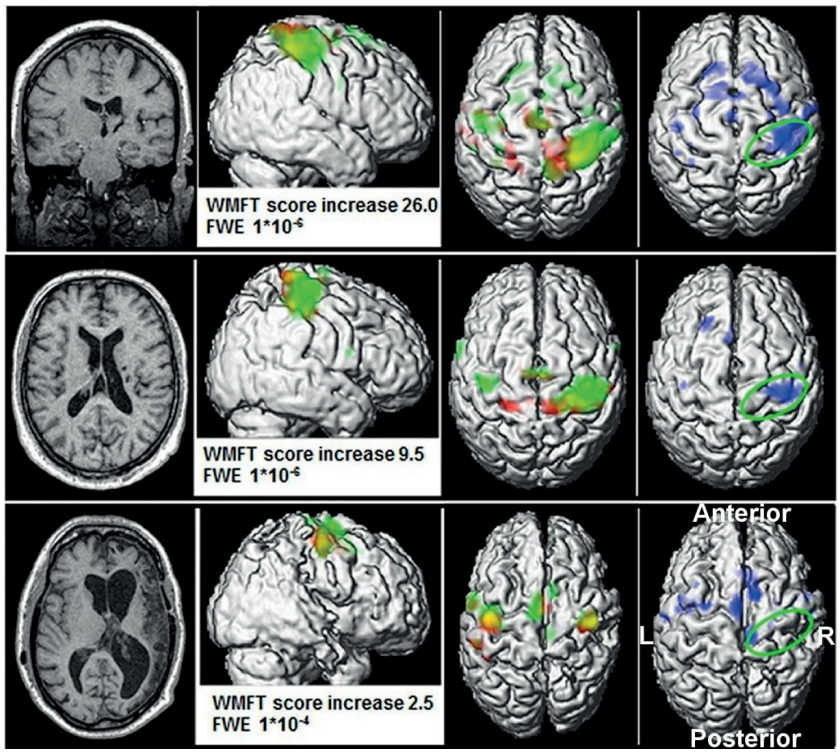

Figure 6.2: *MRIs and fMRI results from three illustrative cases with right hemisphere lesion: Individual lesions (left column) and activation patterns for the paretic hand task before (red) and after (green) rehabilitation (two middle columns). The right column illustrates the therapy-induced increase in activation (blue) and the motor area on the affected hemisphere is circled. All images are in neurological orientation.*

6.1.4 TMS and its correspondence with fMRI

TMS was performed in all patients except one who had a history of epileptic seizures. MEPs in the contralateral hand muscles could be elicited in seven patients while the affected hemisphere was stimulated. Before CIMT, the latencies of MEPs in contralateral hand muscles elicited from affected hemisphere were longer than from the non-affected hemisphere. After the CIMT intervention, the latency of APB MEP elicited from affected hemisphere shortened significantly ($p = 0.046$).

There were three patients who had no MEPs before therapy; they exhibited the three lowest scores and the longest time in WMFT both before and after therapy. The volume of the

increased fMRI activation was significantly larger in patients without MEPs than in patients with MEPs before CIMT.

6.2 ALTERED MOTOR ACTIVATION IN EPM1 PATIENTS (STUDY III)

All 15 patients could perform the flexion/extension motor task according to the instructions, but two patients needed an additional motivational gentle touch because they suffered problems with initiation of movements. Group analysis using the predefined M1 ROI mask revealed decreased activation in the patient group at the left inferior frontal junction (IFJ), (112 voxels; Talairach coordinates -50, 9, 31) (See Figure 6.3).

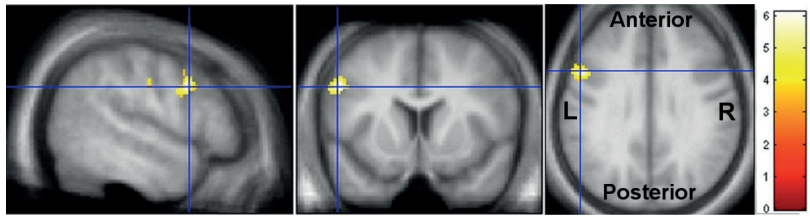

Figure 6.3: *fMRI result of the group comparison. The combination of all individual M1 ROIs was used to mask the T-value map in the group analysis. EPM1 patients have decreased activation at the left inferior frontal junction (uncorrected p<0.001). Images are in neurological orientation. The colour bar shows the scale of T-value.*

In the quantitative analysis of activations, EPM1 patients had lower maximum T-value in the hand knob ROI than the controls ($p = 0.040$). Furthermore, they also displayed lower T-values in bilateral SMA ($p = 0.011$ for mean T-value and $p = 0.024$ for maximum T-value). The quantitative parameters of activations are shown in Table 6.3.

Table 6.3: *fMRI results. The number of voxels N with positive T-value, mean and maximum of T-values in different ROIs are shown in EPM1 patient and control groups as the mean value and the standard deviation in parentheses. Significant group difference (p<0.05) is symbolized with an asterisk.*

	EPM1 patients			Controls		
ROI	**N of vox**	**Max T**	**Mean T**	**N of vox**	**Max T**	**Mean T**
M1	1623	10.48	2.89	1691	11.45	3.10
	(156)	(2.33)	(0.95)	(246)	(2.22)	(0.50)
Hand knob	388	9.42*	4.37	418	11.01	5.47
	(93)	(2.89)	(1.79)	(120)	(2.32)	(1.31)
S1	1055	7.44	2.28	1165	9.57	2.92
	(221)	(3.02)	(1.17)	(241)	(2.38)	(0.79)
SMA	1628	5.34*	1.26*	1785	6.53	1.77
	(441)	(1.21)	(0.41)	(601)	(1.78)	(0.62)

ROI: Region-of-interest, N of vox: Number of voxels, Max T: Maximum of T-value, Mean T: Mean of T-value, M1: primary motor area, S1: primary somatosensory area, SMA: Supplementary motor area

In the EPM1 patients, the higher T-value parameters in SMA were associated with shorter disease durations (the mean of T-value: r = -0.581, p = 0.023; the maximum of T-value: r = -0.592, p = 0.020). The T-value parameters of the patients correlated negatively also with age, whereas no such correlation was seen in the controls. In the EPM1 group, the number of activated voxels in M1 correlated negatively with the duration of disease (r = -0.671, p = 0.006) and with age (r = -0.705, p = 0.003). On the contrary, in the controls, the number of activated voxels in M1 correlated positively with age (r = 0.574, p = 0.025).

6.3 MAPPING OF MOTOR SPEECH AREAS USING NAVIGATED RTMS AND FMRI IN HEALTHY VOLUNTEERS (STUDY IV)

6.3.1 Speech disruptions with rTMS

rTMS elicited sensorimotor activations in all of the subjects and in both hemispheres, although elicited speech arrest was more frequent during stimulations on the left hemisphere. With the left hemisphere stimulations, all but one of the subjects expressed subjective experiences attributable to nTMS induced

effects on speech, which were verified by both reviewers (Category 1 or 2). On the right hemisphere, three subjects experienced subjective speech disruptions and these were verified by both reviewers (Category 2).

The anatomical locations of stimulations with speech disruption varied individually. Most of the verified effective stimulation locations were anterior to the central sulcus, in the precentral gyrus and posterior middle frontal gyrus. In two subjects, the stimulations of the right hemisphere were also extended to the temporal lobe, because they reported possible speech disruptions from extended stimulation areas.

The level of experienced pain or the stimulation intensity did not affect the subjective evaluations of speech disturbance, although the level of pain correlated significantly with the stimulation intensity ($r = 0.196$, $p < 0.001$).

6.3.2 Combination of navigated rTMS and fMRI

The fMRI activation for WGEN was lateralized to the left hemisphere according to LI in eight subjects with one exhibiting bilateral dominance.

The locations of rTMS bursts with subjective experience were more widely distributed than the extent of fMRI activation on the left hemisphere. When the reviewers' confirmations for disturbed speech were taken into account, visual inspection placed the locations of distractive rTMS bursts as following the areas of fMRI activation on the left hemisphere (Figure 6.4). No such similar pattern was observed on the right hemisphere (Figure 6.4).

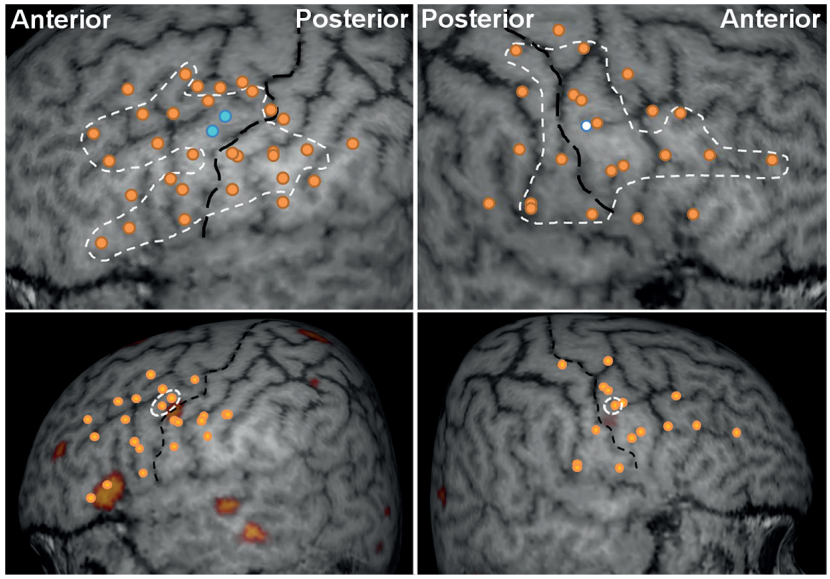

Figure 6.4: *rTMS results. A representative case: In the upper panel, the locations of all stimulation bursts are shown on the left and right hemisphere. The locations of subjective experiences of speech disruption are encircled with the white dashed line, the blue dot denotes reviewer's response Category 2 and the white dot designates the reviewer's response Category 3. In the lower panel the fMRI activations of word generation task (T-value map, threshold uncorrected p-value less than 0.001) are shown on the left and right hemisphere. The locations of stimulation bursts with subject's experience of definitive speech disruption are shown as orange dots and the stimulus locations of at least one reviewer-verified speech disruptions are encircled with the white dashed line. The central sulcus is enhanced with the black dashed line.*

7 Discussion

This thesis consists of four studies published between the years 2005 and 2015. The studies have been carried out in a hospital environment and have a clinical emphasis. The applicability of clinical neuroimaging tools to measure changes in brain activation or perfusion was evaluated. In addition, a multimodal approach was used to discern the brain areas responsible to motor and language processes in overt speech production.

7.1 DETECTION OF CHANGES IN FUNCTIONALITY OF MOTOR AREA IN STROKE PATIENTS

In longitudinal studies, the interest is often focussed on any putative change in the measured variable. Especially with pathological states, it might not be possible to clarify whether the detected increase/decrease is indicative of a normalization of some hypo/hyper condition or the acceleration/inhibition of the baseline condition. The conclusions need to be interpreted based on the direction of the change and on the correlation between measured change and clinical parameters.

In Studies **I** and **II**, the therapy-induced improvements in motor function of stroke patients' paretic hands were accompanied by changes in SPET, fMRI, and TMS parameters. SPET gave valuable information on the changes occurring in cerebral perfusion of motor related areas. The correlation between quantitative fMRI parameters and the clinical parameters are support for the application of fMRI as a tool in rehabilitation follow-up, but more validation will be needed for applications at the individual level. In addition to TMS induced MEPs, there are available other TMS-related measures such as those which measure inhibition or excitability of motor cortex.

CIMT is an exercise rehabilitation program that has been shown to improve the motor recovery of the paretic upper extremity in chronic stroke patients with mild to moderate hemiparesis [92, 115, 165, 167]. Experiments conducted in primate stroke models have demonstrated that structural and functional neural reorganization can occur after extensive training in the early period of rehabilitation after a stroke [121, 134]. The stroke patients in this CIMT rehabilitation program were studied before and after a two week CIMT period, and the motor function in their paretic upper extremities improved significantly due to therapy.

At the group level, the SPET showed increased resting cerebral perfusion in several motor control related areas, not only in the affected hemisphere but also in the non-affected hemisphere. These brain areas receive and integrate the information from different sensory systems and plan the execution of the movement [59, 73, 186]. The increase in perfusion also in the healthy hemisphere may be evidence of bilateral participation in voluntary movement execution. In general, changes in cerebral perfusion reflect alterations in the underlying neuronal activity which may be a sign of an active ongoing reorganization processes. The result of this study revealed some of the cortical areas which may be involved in the reorganization attributable to therapy.

In this study, SPET provided valuable information on changes in perfusion on the cerebral areas associated to motor function. However, nowadays SPET in cerebral perfusion imaging has been mostly replaced by MRI, with methods like contrast enhanced perfusion or arterial spin labeling, or by PET with FDG.

The changes in cortical fMRI activation correlated significantly with the clinical improvement of the paretic hand function. The correlation between SM1 activation for paretic hand task and clinical improvement can be interpreted as reflecting the reorganization occurring in the cortex in the affected hemisphere. In addition to fMRI, TMS was performed to assess cortical plasticity and integrity of motor pathways.

Increased corticospinal conductivity measured by MEP latency was associated with CIMT, but no correlation was found between fMRI parameters and MEPs.

The correlation between longitudinal changes in quantitative fMRI parameters and the clinical parameters support the use of fMRI not only as a research tool, but as a tool for individual follow-up, more validation will be needed. In addition to the MEPs used in this study, there are several other TMS-related measures which could be investigated. The paired-pulse TMS, the silent period, and the motor threshold are believed to reflect the neurophysiological properties of the motor area. Paired-pulse TMS elicits inhibition or excitation of MEP amplitude depending on inter-stimulus-interval of pulses. The inhibitory silent period is a transient suppression of voluntary muscle activity seen in EMG after TMS. And furthermore, the nTMS allows repetition of the stimulation in an anatomically identical location even in longitudinal studies, which improves the technique's repeatability.

7.2 ALTERED MOTOR ACTIVATION IN EPM1 PATIENTS

In Study **III**, an fMRI examination was used to clarify whether cortical activation related to a motor task was altered in EPM1 patients. The quantitative fMRI results showed weaker activation in the motor areas of EPM1 patients than in their controls. The patients had also less activation in IFJ than the controls. This weakening in motor related activations may be associated with the motor symptoms encountered in EPM1.

The patients had weaker activation at the hand knob and bilateral SMA than controls. In structural studies, atrophy has been found in the sensorimotor area and SMA [85] and there is also a thinner cortex in the sensorimotor area [86]. These structural changes in EPM1 patients may support the concept that a smaller population of neurons elicits weaker activation or alternatively the observed weaker increase of BOLD may be attributable to either the increased baseline cortical excitation

[76, 78] or decreased activation during motor task as a consequence of cortical inhibition [34]. Thus, the observed decrease in activation of IFJ area in EPM1 patients may be associated with their difficulties in initiation or termination of motor execution, a typical clinical symptom in EPM1. The fMRI findings in this study reflect the progressive nature of this disease.

Altered motor fMRI activations were found with simple motor task, and these results were in parallel with previous structural and neurophysiological findings and correlated with the motor symptoms of the disease.

7.3 SEPARATION OF MOTOR SPEECH AREAS FROM LANGUAGE AREAS IN HEALTHY VOLUNTEERS

The functional neuroanatomy of speech and language is complex. Language depends on several different processes, such as storage of words in short-term memory, phonologic, and semantic processing in relation to the lexicon in long-term memory, arranging words into sentences, and issuing of commands to motor areas to produce audible speech [19]. Whereas navigated rTMS created discrete virtual lesions in the speech and language network, the area of interest was tested point by point on both hemispheres. Speech was disrupted also during right hemisphere stimulations, indicating that some of the disruptions had originated from motor speech areas. This multimodal neuroimaging approach makes it possible to separate some of the different processes involved in speech and language.

Navigated rTMS has been increasingly used in research investigating functional language areas. The method mimics direct cortical stimulation but it has the advantage of non-invasiveness and also the longer available examination time than can be attained with DCS in awake craniotomy. Object naming has been used as task in most navigated rTMS studies resulting in momentary aphasia or lexical errors [63, 75, 76, 90,

103, 131, 152-155]. In addition, the ongoing speech can be disrupted by rTMS, probably by causing motor arrest or aphasia. More tasks than object naming or fluent speech would be needed if one wished to separate the different language processes such as planning and executing speech, identification of linguistic processes, auditory processing of speech.

rTMS can easily disturb both the language processes and the motor execution of speech at the same time. To further differentiate whether the rTMS disturbed the motor output of speech (arrest) or the language process itself (aphasia), another functional examination method, like fMRI, should be utilized. The WGEN task in particular has been shown to produce robust language localization and highly lateralized fMRI results [17, 104, 127, 194]. The high degree of laterality seen in WGEN tasks has been thought to be related to language production. It has been shown that when compared to DCS, rTMS is less affected by a brain lesion than fMRI [75] but the combination of these techniques has resulted in a higher correlation than can be obtained with either of the techniques alone [76].

The reviewer-verified speech disruptions induced by navigated rTMS provided clinically relevant information, and fMRI might further clarify the function of the cortical area. Navigated rTMS and fMRI complement each other, and their combination can be advocated if one wishes to evaluate the localization of the speech network in an individual subject. Nonetheless, further development of the methods will still be needed to understand better the functional neuroanatomy of speech and language.

7.4 FUTURE ASPECTS

Research and development of the present neuroimaging methods will improve further the sensitivity and accuracy of the methods, and may even produce totally new methods. The higher magnetic fields assist fMRI by providing better contrast, better resolution, and faster imaging, but also add vulnerability

to artefacts. The development of arterial spin labeling method in MRI will implement perfusion imaging without the need for contrast medium. It is likely that advances in resting state fMRI will shed light on neural networks in the background of cerebral disorders without focal clinical symptoms. The wider availability of more sensitive PET and SPET tracers and local cyclotrons will lead to the technique's greater clinical exploitation for assessing cerebral perfusion. Transcranial magnetic stimulation will undoubtedly benefit from advances in multi-coil systems and the development of new pulse forms or trains. The increasing computing capacity makes it possible to collect and analyse ever greater amounts of data, which may make possible the elucidation of neural networks during rest and life-like stimulations, as well as the creation of databases for facilitating diagnostics. In hospitals, there is a need to be open-minded and tireless when implementing, testing, and validating these new methods for clinical work.

Adoption of a multimodal approach in functional brain examination is an asset. Brain functions are complex and it is necessary to utilize a multimodal approach if one wishes to characterize the distinct brain areas. Functional brain imaging measures may serve as objective biomarkers and indexes of brain states and help in monitoring the effects of disease and therapy. Information from functional imaging may eventually guide patient selection and aid in the design of treatments.

8 Conclusions

In the present thesis, the feasibility of different clinical neuroimaging tools to measure changes in brain activation or perfusion was evaluated.

1. The clinical neuroimaging methods used in this study detected longitudinal changes in the function of the motor area following therapy. The changes correlated with the improvements in hand function.
2. In a cross-sectional study, block design fMRI examination found altered motor activations in EPM1 patients. The results paralleled previous structural and neuro-physiological findings and correlated with the motor symptoms of the disease.
3. By adopting a multimodal approach, it was found that the reviewer-verified navigated rTMS mapping of speech areas provided clinically relevant information, and fMRI helped to clarify the function of the cortical area being affected. Further development of the clinical methods will be needed to separate the distinctive language specific areas from each other.
4. At the group level, the clinical examination methods used in this study were capable of detecting changes in motor related cortical activation.
5. At the individual level, the detected changes in fMRI activation alone cannot be applied in the prediction or follow-up of disease, and thus further development of the methods is needed. However, the adoption of a multimodal approach of fMRI and TMS does improve the reliability of functional mapping.

References

[1] Aaslid R., Lindegaard K. F., Sorteberg W., Nornes H., "Cerebral autoregulation dynamics in humans", *Stroke* **20,** 45-52 (1989).

[2] Abbott N. J., Ronnback L., Hansson E., "Astrocyte-endothelial interactions at the blood-brain barrier", *Nat Rev Neurosci* **7,** 41-53 (2006).

[3] Anger H. O., "Scintillation camera", *Rev Sci Instr* **29,** 27-33 (1958).

[4] Aquirre G. K. Experimental design and data analysis for fMRI. In: Faro S. H., Mohamed F. B., eds. *Functional MRI Basic Principles and Clinical Applications*. New York: Springer, 2006: 58-74.

[5] Aziz-Zadeh L., Cattaneo L., Rochat M., Rizzolatti G., "Covert speech arrest induced by rTMS over both motor and nonmotor left hemisphere frontal sites", *J Cogn Neurosci* **17,** 928-938 (2005).

[6] Barker A. T., Jalinous R., Freeston I. L., "Non-invasive magnetic stimulation of human motor cortex", *Lancet* **1,** 1106-1107 (1985).

[7] Basser P. J., Roth B. J., "Stimulation of a myelinated nerve axon by electromagnetic induction", *Med Biol Eng Comput* **29,** 261-268 (1991).

[8] Behroozmand R., Shebek R., Hansen D. R., Oya H., Robin D. A., Howard M. A., 3rd, Greenlee J. D., "Sensory-motor networks involved in speech production and motor control: an fMRI study", *Neuroimage* **109,** 418-428 (2015).

[9] Belliveau J. W., Kennedy D. N., Jr., McKinstry R. C., Buchbinder B. R., Weisskoff R. M., Cohen M. S., Vevea J. M., Brady T. J., Rosen B. R., "Functional mapping of the human visual cortex by magnetic resonance imaging", *Science* **254,** 716-719 (1991).

[10] Belyaev A. S., Peck K. K., Brennan N. M., Holodny A. I., "Clinical applications of functional MR imaging", *Magn Reson Imaging Clin N Am* **21,** 269-278 (2013).

[11] Binder J. R., Frost J. A., Hammeke T. A., Cox R. W., Rao S. M., Prieto T., "Human brain language areas identified by functional magnetic resonance imaging", *J Neurosci* **17,** 353-362 (1997).

[12] Bizzi A., Blasi V., Falini A., Ferroli P., Cadioli M., Danesi U., Aquino D., Marras C., Caldiroli D., Broggi G., "Presurgical

functional MR imaging of language and motor functions: validation with intraoperative electrocortical mapping", *Radiology* **248,** 579-589 (2008).

[13] Blatow M., Reinhardt J., Riffel K., Nennig E., Wengenroth M., Stippich C., "Clinical functional MRI of sensorimotor cortex using passive motor and sensory stimulation at 3 Tesla", *J Magn Reson Imaging* **34,** 429-437 (2011).

[14] Bloch F., "Nuclear induction", *Phys Rev* **70,** 460-474 (1946).

[15] Borich M. R., Brodie S. M., Gray W. A., Ionta S., Boyd L. A., "Understanding the role of the primary somatosensory cortex: opportunities for rehabilitation", *Neuropsychologia***,** Epub ahead of print (2015).

[16] Bosnell R., Wegner C., Kincses Z. T., Korteweg T., Agosta F., Ciccarelli O., De Stefano N., Gass A., Hirsch J., Johansen-Berg H., Kappos L., Barkhof F., Mancini L., Manfredonia F., Marino S., Miller D. H., Montalban X., Palace J., Rocca M., Enzinger C., Ropele S., Rovira A., Smith S., Thompson A., Thornton J., Yousry T., Whitcher B., Filippi M., Matthews P. M., "Reproducibility of fMRI in the clinical setting: implications for trial designs", *Neuroimage* **42,** 603-610 (2008).

[17] Brannen J. H., Badie B., Moritz C. H., Quigley M., Meyerand M. E., Haughton V. M., "Reliability of functional MR imaging with word-generation tasks for mapping Broca's area", *AJNR Am J Neuroradiol* **22,** 1711-1718 (2001).

[18] Broca P., "Remarques sur le sie`ge de la faculte´ du langage articule´; suivies d'une observation d'aphemie", *Bull Soc Anat Paris* **6,** 330-357 (1861).

[19] Brodal P., *The Central Nervous System: Structure and Function*, 3rd edn. New York: Oxford University Press, Inc., 2004.

[20] Brodmann K., *Vergleichende lokalisationslehre der großhirnrinde*. Leipzig: Verlag von Johann Ambrosius Barth, 1909.

[21] Brust J. C. M. Circulation of the brain. In: Kandel E. R., Schwartz J. H., Jessell T. M., eds. *Principles of Neural Science*. 4th edn. Connecticut: The McGraw-Hill Companies, Inc, 2000: 1302-1316.

[22] Buxton R. B., "The elusive initial dip", *Neuroimage* **13,** 953-958 (2001).

[23] Buxton R. B., *Introduction to Functional Magnetic Resonance Imaging Principles and Techniques*, 2nd edn. New York: Cambridge University Press, 2009.

[24] Cacchio A., Paoloni M., Cimini N., Mangone M., Liris G., Aloisi P., Santilli V., Marrelli A., "Reliability of TMS-related measures of tibialis anterior muscle in patients with chronic stroke and healthy subjects", *J Neurol Sci* **303,** 90-94 (2011).

[25] Catani M., Jones D. K., ffytche D. H., "Perisylvian language networks of the human brain", *Ann Neurol* **57,** 8-16 (2005).

[26] Chang C. H., "A method for attenuation correction in radiounclide computed tomography", *IEEE Trans Nucl Sci* **NS-25,** 638-643 (1978).

[27] Chen B. R., Bouchard M. B., McCaslin A. F., Burgess S. A., Hillman E. M., "High-speed vascular dynamics of the hemodynamic response", *Neuroimage* **54,** 1021-1030 (2011).

[28] Cherry S. R., Sorenson J. A., Phelps M. E., *Physics in Nuclear Medicine*, 4th edn. Philadelphia: Elsevier, 2012.

[29] Chez C., Gordon J. An introduction to movement. In: Kandel E. R., Schwartz J. H., Jessell T. M., eds. *Essentials of Neural Science and Behavior*. Connecticut: Appelton & Lange, 1995: 489-500.

[30] Cox R. W., "AFNI: software for analysis and visualization of functional magnetic resonance neuroimages", *Comput Biomed Res* **29,** 162-173 (1996).

[31] Crinion J., Ashburner J., Leff A., Brett M., Price C., Friston K., "Spatial normalization of lesioned brains: performance evaluation and impact on fMRI analyses", *Neuroimage* **37,** 866-875 (2007).

[32] D'Olhaberriague L., Hernandez-Vidal A., Molina L., Soler-Singla L., Marrugat J., Pons S., Moral A., Pou-Serradell A., "A prospective study of atrial fibrillation and stroke", *Stroke* **20,** 1648-1652 (1989).

[33] Danner N., Julkunen P., Hyppönen J., Hukkanen T., Könönen M., Säisänen L., Koskenkorva P., Vanninen R., Lehesjoki A. E., Kälviäinen R., Mervaala E., "Altered cortical inhibition in Unverricht-Lundborg type progressive myoclonus epilepsy (EPM1)", *Epilepsy Res* **85,** 81-88 (2009).

[34] Danner N., Julkunen P., Hyppönen J., Niskanen E., Säisänen L., Könönen M., Koskenkorva P., Vanninen R., Kälviäinen R., Mervaala E., "Alterations of motor cortical excitability and

anatomy in Unverricht-Lundborg disease", *Mov Disord* **28,** 1860-1867 (2013).

[35] Danner N., Säisänen L., Määttä S., Julkunen P., Hukkanen T., Könönen M., Hyppönen J., Kälviäinen R., Mervaala E., "Motor cortical plasticity is impaired in Unverricht-Lundborg disease", *Mov Disord* **26,** 2095-2100 (2011).

[36] Detre J. A., Alsop D. C., "Perfusion magnetic resonance imaging with continuous arterial spin labeling: methods and clinical applications in the central nervous system", *Eur J Radiol* **30,** 115-124 (1999).

[37] Detre J. A., Wang J., Wang Z., Rao H., "Arterial spin-labeled perfusion MRI in basic and clinical neuroscience", *Curr Opin Neurol* **22,** 348-355 (2009).

[38] Devlin J. T., Watkins K. E., "Stimulating language: insights from TMS", *Brain* **130,** 610-622 (2007).

[39] Di Lazzaro V., Oliviero A., Pilato F., Saturno E., Dileone M., Mazzone P., Insola A., Tonali P. A., Rothwell J. C., "The physiological basis of transcranial motor cortex stimulation in conscious humans", *Clin Neurophysiol* **115,** 255-266 (2004).

[40] Di Lazzaro V., Oliviero A., Profice P., Saturno E., Pilato F., Insola A., Mazzone P., Tonali P., Rothwell J. C., "Comparison of descending volleys evoked by transcranial magnetic and electric stimulation in conscious humans", *Electroencephalogr Clin Neurophysiol* **109,** 397-401 (1998).

[41] Di Lazzaro V., Oliviero A., Saturno E., Pilato F., Insola A., Mazzone P., Profice P., Tonali P., Rothwell J. C., "The effect on corticospinal volleys of reversing the direction of current induced in the motor cortex by transcranial magnetic stimulation", *Exp Brain Res* **138,** 268-273 (2001).

[42] Di Lazzaro V., Ziemann U., Lemon R. N., "State of the art: Physiology of transcranial motor cortex stimulation", *Brain Stimul* **1,** 345-362 (2008).

[43] Dick A. S., Tremblay P., "Beyond the arcuate fasciculus: consensus and controversy in the connectional anatomy of language", *Brain* **135,** 3529-3550 (2012).

[44] Epstein C. M. Physics and biophysics of TMS. In: Wassermann E. M., Epstein C. M., Ziemann U., Walsh V., Paus T., Lisanby S. H.,

eds. *The Oxford Handbook of Transcranial Stimulation*. New York: Oxford University Press, 2008: 3-74.

[45] Epstein C. M., Meador K. J., Loring D. W., Wright R. J., Weissman J. D., Sheppard S., Lah J. J., Puhalovich F., Gaitan L., Davey K. R., "Localization and characterization of speech arrest during transcranial magnetic stimulation", *Clin Neurophysiol* **110,** 1073-1079 (1999).

[46] Feigin V. L., Forouzanfar M. H., Krishnamurthi R., Mensah G. A., Connor M., Bennett D. A., Moran A. E., Sacco R. L., Anderson L., Truelsen T., O'Donnell M., Venketasubramanian N., Barker-Collo S., Lawes C. M., Wang W., Shinohara Y., Witt E., Ezzati M., Naghavi M., Murray C., "Global and regional burden of stroke during 1990-2010: findings from the Global Burden of Disease Study 2010", *Lancet* **383,** 245-254 (2010).

[47] Fellner C., Doenitz C., Finkenzeller T., Jung E. M., Rennert J., Schlaier J., "Improving the spatial accuracy in functional magnetic resonance imaging (fMRI) based on the blood oxygenation level dependent (BOLD) effect: benefits from parallel imaging and a 32-channel head array coil at 1.5 Tesla", *Clin Hemorheol Microcirc* **43,** 71-82 (2009).

[48] Ferlazzo E., Magaudda A., Striano P., Vi-Hong N., Serra S., Genton P., "Long-term evolution of EEG in Unverricht-Lundborg disease", *Epilepsy Res* **73,** 219-227 (2007).

[49] Ferro J. M., "Cardioembolic stroke: an update", *Lancet Neurol* **2,** 177-188 (2003).

[50] Flitman S. S., Grafman J., Wassermann E. M., Cooper V., O'Grady J., Pascual-Leone A., Hallett M., "Linguistic processing during repetitive transcranial magnetic stimulation", *Neurology* **50,** 175-181 (1998).

[51] Forster M. T., Hattingen E., Senft C., Gasser T., Seifert V., Szelenyi A., "Navigated transcranial magnetic stimulation and functional magnetic resonance imaging: advanced adjuncts in preoperative planning for central region tumors", *Neurosurgery* **68,** 1317-1324; discussion 1324-1315 (2011).

[52] Friston K. J., Holmes A. P., Poline J. B., Grasby P. J., Williams S. C., Frackowiak R. S., Turner R., "Analysis of fMRI time-series revisited", *Neuroimage* **2,** 45-53 (1995).

[53] Friston K. J., Williams S., Howard R., Frackowiak R. S., Turner R., "Movement-related effects in fMRI time-series", *Magn Reson Med* **35,** 346-355 (1996).

[54] Frucht S. J., Leurgans S. E., Hallett M., Fahn S., "The Unified Myoclonus Rating Scale", *Adv Neurol* **89,** 361-376 (2002).

[55] Galhardoni R., Correia G. S., Araujo H., Yeng L. T., Fernandes D. T., Kaziyama H. H., Marcolin M. A., Bouhassira D., Teixeira M. J., de Andrade D. C., "Repetitive transcranial magnetic stimulation in chronic pain: A review of the literature", *Arch Phys Med Rehabil* **96,** S156-S172 (2015).

[56] Garey L. J., *BRODMANN'S Localisation in the cerebral cortex*, 3rd edn. New York: Spinger Science+Business Media, 2010.

[57] Gaynes B. N., Lloyd S. W., Lux L., Gartlehner G., Hansen R. A., Brode S., Jonas D. E., Swinson Evans T., Viswanathan M., Lohr K. N., "Repetitive transcranial magnetic stimulation for treatment-resistant depression: a systematic review and meta-analysis", *J Clin Psychiatry* **75,** 477-489 (2014).

[58] Genovese C. R., Lazar N. A., Nichols T., "Thresholding of statistical maps in functional neuroimaging using the false discovery rate", *Neuroimage* **15,** 870-878 (2002).

[59] Grafton S. T., Arbib M. A., Fadiga L., Rizzolatti G., "Localization of grasp representations in humans by positron emission tomography. 2. Observation compared with imagination", *Exp Brain Res* **112,** 103-111. (1996).

[60] Hajnal J. V., Myers R., Oatridge A., Schwieso J. E., Young I. R., Bydder G. M., "Artifacts due to stimulus correlated motion in functional imaging of the brain", *Magn Reson Med* **31,** 283-291 (1994).

[61] Hallett M., "Transcranial magnetic stimulation: a primer", *Neuron* **55,** 187-199 (2007).

[62] Hara Y., "Brain plasticity and rehabilitation in stroke patients", *J Nippon Med Sch* **82,** 4-13 (2015).

[63] Hauck T., Tanigawa N., Probst M., Wohlschlaeger A., Ille S., Sollmann N., Maurer S., Zimmer C., Ringel F., Meyer B., Krieg S. M., "Task type affects location of language-positive cortical regions by repetitive navigated transcranial magnetic stimulation mapping", *PLoS One* **10,** e0125298 (2015).

[64] Hess C. W. Central motor conduction and its clinical applications. In: Hallet M., Chokroverty S., eds. *Magnetic stimulation in clinical neurophysiology*. 2nd edn. Philadelphia: Elsevier, 2005: 83-103.

[65] Hickok G., Poeppel D., "The cortical organization of speech processing", *Nat Rev Neurosci* **8,** 393-402 (2007).

[66] Hillman E. M., "Coupling mechanism and significance of the BOLD signal: a status report", *Annu Rev Neurosci* **37,** 161-181 (2014).

[67] Hillman E. M., Devor A., Bouchard M. B., Dunn A. K., Krauss G. W., Skoch J., Bacskai B. J., Dale A. M., Boas D. A., "Depth-resolved optical imaging and microscopy of vascular compartment dynamics during somatosensory stimulation", *Neuroimage* **35,** 89-104 (2007).

[68] Hof P. R., Trapp B. D., de Vellis J., Claudio L., Colman D. R. The cellular components of nervous tissue. In: Zigmond L. M., Bloom F. E., Landis S. E., Roberts J. L., Squire L. R., eds. *Fundamental Neuroscience*. London: Academic Press, 1999.

[69] Hosp J. A., Luft A. R., "Cortical plasticity during motor learning and recovery after ischemic stroke", *Neural Plast* **2011,** 871296 (2011).

[70] Huettel S. A., "Event-related fMRI in cognition", *Neuroimage* **62,** 1152-1156 (2009).

[71] Huettel S. A., Song A. W., McCarthy G., *Functional Magnetic Resonance Imaging*, 2nd edn. Sunderland: Sinauer Associates, 2009.

[72] Huettel S. A., Stowe C. J., Gordon E. M., Warner B. T., Platt M. L., "Neural signatures of economic preferences for risk and ambiguity", *Neuron* **49,** 765-775 (2006).

[73] Ikeda A., Luders H. O., Burgess R. C., Shibasaki H., "Movement-related potentials recorded from supplementary motor area and primary motor area. Role of supplementary motor area in voluntary movements", *Brain* **115,** 1017-1043. (1992).

[74] Iliff J. J., Lee H., Yu M., Feng T., Logan J., Nedergaard M., Benveniste H., "Brain-wide pathway for waste clearance captured by contrast-enhanced MRI", *J Clin Invest* **123,** 1299-1309 (2015).

[75] Ille S., Sollmann N., Hauck T., Maurer S., Tanigawa N., Obermueller T., Negwer C., Droese D., Boeckh-Behrens T., Meyer B., Ringel F., Krieg S. M., "Impairment of preoperative language mapping by lesion location: a functional magnetic resonance

imaging, navigated transcranial magnetic stimulation, and direct cortical stimulation study", *J Neurosurg* **123,** 314-324 (2015).

[76] Ille S., Sollmann N., Hauck T., Maurer S., Tanigawa N., Obermueller T., Negwer C., Droese D., Zimmer C., Meyer B., Ringel F., Krieg S. M., "Combined noninvasive language mapping by navigated transcranial magnetic stimulation and functional MRI and its comparison with direct cortical stimulation", *J Neurosurg* **123,** 212-225 (2015).

[77] Ilmoniemi R. J., Ruohonen J., Karhu J., "Transcranial magnetic stimulation--a new tool for functional imaging of the brain", *Crit Rev Biomed Eng* **27,** 241-284 (1999).

[78] Julkunen P., Säisänen L., Könönen M., Vanninen R., Kälviäinen R., Mervaala E., "TMS-EEG reveals impaired intracortical interactions and coherence in Unverricht-Lundborg type progressive myoclonus epilepsy (EPM1)", *Epilepsy Res* **106,** 103-112 (2013).

[79] Kälviäinen R., Khyuppenen J., Koskenkorva P., Eriksson K., Vanninen R., Mervaala E., "Clinical picture of EPM1-Unverricht-Lundborg disease", *Epilepsia* **49,** 549-556 (2008).

[80] Kandel E., Siegelbaum S. Transmission at the nerve-muscle synapse. In: Kandel E. R., Schwartz J. H., Jessell T. M., eds. *Essentials of Neural Science and Behavior*. Connecticut: Appleton & Lange, 1995: 489-500.

[81] Kimberley T. J., Khandekar G., Borich M., "fMRI reliability in subjects with stroke", *Exp Brain Res* **186,** 183-190 (2008).

[82] Klem G. H., Lüders H. O., Jasper H. H., Elger C. The ten-twenty electrode system of the International Federation. In: Deuschl G., Eisen A., eds. *Recommendations for the Practice of Clinical Neurophysiology: Guidelines of the International Federation of Clinical Physiology (EEG Suppl 52)*: Elsevier Science B.V, 1999: 3-6.

[83] Koester J. Propagated signaling: The action potential. In: Kandel E. R., Schwartz J. H., Jessell T. M., eds. *Essentials of Neural Science and Behavior*. Connecticut: Appleton & Lange, 1995: 161-177.

[84] Kolb B., Whishaw I. Q., "Brain plasticity and behavior", *Annu Rev Psychol* **49,** 43-64 (1998).

[85] Koskenkorva P., Khyuppenen J., Niskanen E., Könönen M., Bendel P., Mervaala E., Lehesjoki A. E., Kälviäinen R., Vanninen R., "Motor cortex and thalamic atrophy in Unverricht-Lundborg

disease: voxel-based morphometric study", *Neurology* **73,** 606-611 (2009).

[86] Koskenkorva P., Niskanen E., Hyppönen J., Könönen M., Mervaala E., Soininen H., Kälviäinen R., Vanninen R., "Sensorimotor, visual, and auditory cortical atrophy in Unverricht-Lundborg disease mapped with cortical thickness analysis", *AJNR Am J Neuroradiol* **33,** 878-883 (2012).

[87] Kowalsky R. J., Falen S. W., *Radiopharmaceuticals in Nuclear Pharmacy and Nuclear Medicine,* 2nd edn. Washington: The American Pharmacists Association, 2004.

[88] Krieg S. M., Sabih J., Bulubasova L., Obermueller T., Negwer C., Janssen I., Shiban E., Meyer B., Ringel F., "Preoperative motor mapping by navigated transcranial magnetic brain stimulation improves outcome for motor eloquent lesions", *Neuro Oncol* **16,** 1274-1282 (2014).

[89] Krieg S. M., Shiban E., Buchmann N., Gempt J., Foerschler A., Meyer B., Ringel F., "Utility of presurgical navigated transcranial magnetic brain stimulation for the resection of tumors in eloquent motor areas", *J Neurosurg* **116,** 994-1001 (2012).

[90] Krieg S. M., Sollmann N., Tanigawa N., Foerschler A., Meyer B., Ringel F., "Cortical distribution of speech and language errors investigated by visual object naming and navigated transcranial magnetic stimulation", *Brain Struct Funct***,** Epub ahead of print (2015).

[91] Kuikka J. T., Tenhunen-Eskelinen M., Jurvelin J., Kiiliänen H., "Physical performance of the Siemens MultiSPECT 3 gamma camera", *Nucl Med Commun* **14,** 490-497. (1993).

[92] Kunkel A., Kopp B., Muller G., Villringer K., Villringer A., Taub E., Flor H., "Constraint-induced movement therapy for motor recovery in chronic stroke patients", *Arch Phys Med Rehabil* **80,** 624-628. (1999).

[93] Kwakkel G., Veerbeek J. M., van Wegen E. E., Wolf S. L., "Constraint-induced movement therapy after stroke", *Lancet Neurol* **14,** 224-234 (2015).

[94] Lahnakoski J. M., Glerean E., Jääskeläinen I. P., Hyönä J., Hari R., Sams M., Nummenmaa L., "Synchronous brain activity across individuals underlies shared psychological perspectives", *Neuroimage* **100,** 316-324 (2014).

[95] Langhorne P., Bernhardt J., Kwakkel G., "Stroke rehabilitation", *Lancet* **377,** 1693-1702 (2011).

[96] Langhorne P., Coupar F., Pollock A., "Motor recovery after stroke: a systematic review", *Lancet Neurol* **8,** 741-754 (2009).

[97] Lauterbur P. C., "Image formation by induced local interactions: examples employing nuclear magnetic resonance", *Nature* **242,** 190-191 (1993).

[98] Lehericy S., Duffau H., Cornu P., Capelle L., Pidoux B., Carpentier A., Auliac S., Clemenceau S., Sichez J. P., Bitar A., Valery C. A., Van Effenterre R., Faillot T., Srour A., Fohanno D., Philippon J., Le Bihan D., Marsault C., "Correspondence between functional magnetic resonance imaging somatotopy and individual brain anatomy of the central region: comparison with intraoperative stimulation in patients with brain tumors", *J Neurosurg* **92,** 589-598 (2000).

[99] Lehesjoki A. E., *Clinical features and genetics of Unverricht-Lunborg disease* Philadelphia: Lippincott Williams and Wilkins, 2002.

[100] Lehesjoki A. E., Koskiniemi M., Sistonen P., Miao J., Hastbacka J., Norio R., de la Chapelle A., "Localization of a gene for progressive myoclonus epilepsy to chromosome 21q22", *Proc Natl Acad Sci U S A* **88,** 3696-3699 (1991).

[101] Li X., *Functional Magnetic Resonance Imaging Processing*. Dordrecht: Springer, 2014.

[102] Lindauer U., Leithner C., Kaasch H., Rohrer B., Foddis M., Fuchtemeier M., Offenhauser N., Steinbrink J., Royl G., Kohl-Bareis M., Dirnagl U., "Neurovascular coupling in rat brain operates independent of hemoglobin deoxygenation", *J Cereb Blood Flow Metab* **30,** 757-768 (2010).

[103] Lioumis P., Zhdanov A., Mäkelä N., Lehtinen H., Wilenius J., Neuvonen T., Hannula H., Deletis V., Picht T., Mäkelä J. P., "A novel approach for documenting naming errors induced by navigated transcranial magnetic stimulation", *J Neurosci Methods* **204,** 349-354 (2012).

[104] Mahdavi A., Houshmand S., Oghabian M. A., Zarei M., Mahdavi A., Shoar M. H., Ghanaati H., "Developing optimized fMRI protocol for clinical use: comparison of different language paradigms", *J Magn Reson Imaging* **34,** 413-419 (2011).

[105] Majos A., Tybor K., Stefanczyk L., Goraj B., "Cortical mapping by functional magnetic resonance imaging in patients with brain tumors", *Eur Radiol* **15,** 1148-1158 (2005).

[106] Mangraviti A., Casali C., Cordella R., Legnani F. G., Mattei L., Prada F., Saladino A., Contarino V. E., Perin A., DiMeco F., "Practical assessment of preoperative functional mapping techniques: navigated transcranial magnetic stimulation and functional magnetic resonance imaging", *Neurol Sci* **34,** 1551-1557 (2013).

[107] Mansfield P., Maudsley A. A., "Planar spin imaging by NMR", *J Magn Reson Imaging* **27,** 101-119 (1977).

[108] Marshall I., Simonotto E., Deary I. J., Maclullich A., Ebmeier K. P., Rose E. J., Wardlaw J. M., Goddard N., Chappell F. M., "Repeatability of motor and working-memory tasks in healthy older volunteers: assessment at functional MR imaging", *Radiology* **233,** 868-877 (2004).

[109] Martindale J., Mayhew J., Berwick J., Jones M., Martin C., Johnston D., Redgrave P., Zheng Y., "The hemodynamic impulse response to a single neural event", *J Cereb Blood Flow Metab* **23,** 546-555 (2003).

[110] Mazziotta J., Toga A., Evans A., Fox P., Lancaster J., Zilles K., Woods R., Paus T., Simpson G., Pike B., Holmes C., Collins L., Thompson P., MacDonald D., Iacoboni M., Schormann T., Amunts K., Palomero-Gallagher N., Geyer S., Parsons L., Narr K., Kabani N., Le Goualher G., Boomsma D., Cannon T., Kawashima R., Mazoyer B., "A probabilistic atlas and reference system for the human brain: International Consortium for Brain Mapping (ICBM)", *Philos Trans R Soc Lond B Biol Sci* **356,** 1293-1322 (2001).

[111] McCormic D. A. Membrane potential and action potential. In: Zigmond M. J., Bloom F. E., Landis S. C., Roberts J. L., Squire L. R., eds. *Fundamental Neuroscience*. London: Academic Press, 1999: 129-154.

[112] Mehta A. D., Klein G., "Clinical utility of functional magnetic resonance imaging for brain mapping in epilepsy surgery", *Epilepsy Res* **89,** 126-132 (2010).

[113] Merton P. A., Morton H. B., "Stimulation of the cerebral cortex in the intact human subject", *Nature* **285,** 227 (1980).

[114] Mettler F. A. J., Guiberteau M. J., *Essentials of Nuclear Medicine Imaging*, 6th edn. Philadelphia: Elsevier, 2012.

[115] Miltner W. H., Bauder H., Sommer M., Dettmers C., Taub E., "Effects of constraint-induced movement therapy on patients with chronic motor deficits after stroke: a replication", *Stroke* **30,** 586-592. (1999).

[116] Natsubori T., Hashimoto R., Yahata N., Inoue H., Takano Y., Iwashiro N., Koike S., Gonoi W., Sasaki H., Takao H., Abe O., Kasai K., Yamasue H., "An fMRI study of visual lexical decision in patients with schizophrenia and clinical high-risk individuals", *Schizophr Res* **157,** 218-224 (2014).

[117] Nichols T., Hayasaka S., "Controlling the familywise error rate in functional neuroimaging: a comparative review", *Stat Methods Med Res* **12,** 419-446 (2003).

[118] Niehaus L., Meyer B. U., Weyh T., "Influence of pulse configuration and direction of coil current on excitatory effects of magnetic motor cortex and nerve stimulation", *Clin Neurophysiol* **111,** 75-80 (2000).

[119] Niskanen E., Könönen M., Villberg V., Nissi M., Ranta-Aho P., Säisänen L., Karjalainen P., Äikiä M., Kälviäinen R., Mervaala E., Vanninen R., "The effect of fMRI task combinations on determining the hemispheric dominance of language functions", *Neuroradiology* **54,** 393-405 (2012).

[120] Nudo R. J., Milliken G. W., Jenkins W. M., Merzenich M. M., "Use-dependent alterations of movement representations in primary motor cortex of adult squirrel monkeys", *J Neurosci* **16,** 785-807 (1996).

[121] Nudo R. J., Wise B. M., SiFuentes F., Milliken G. W., "Neural substrates for the effects of rehabilitative training on motor recovery after ischemic infarct", *Science* **272,** 1791-1794. (1996).

[122] Ogawa S., Lee T. M., Nayak A. S., Glynn P., "Oxygenation-sensitive contrast in magnetic resonance image of rodent brain at high magnetic fields", *Magn Reson Med* **14,** 68-78 (1990).

[123] Ojakangas C. L., Donoghue J. P. Plasticity of cerebral motor functions: implications for repair and rehabilitation. In: Selzer M. E., Clarke S., Cohen L. G., Duncan P. W., Gage F. H., eds. *Textbook of Neural Repair and Rehabilitation*. New York: Cambridge University Press, 2006: 126-146.

[124] Oldfield R. C., "The assessment and analysis of handedness: the Edinburgh inventory", *Neuropsychologia* **9,** 97-113 (1971).
[125] Ordidge R. J., Mansfield P., Coupland R. E., "Rapid biomedical imaging by NMR", *Br J Radiol* **54,** 850-855 (1981).
[126] Parker G. J., Luzzi S., Alexander D. C., Wheeler-Kingshott C. A., Ciccarelli O., Lambon Ralph M. A., "Lateralization of ventral and dorsal auditory-language pathways in the human brain", *Neuroimage* **24,** 656-666 (2005).
[127] Partovi S., Konrad F., Karimi S., Rengier F., Lyo J. K., Zipp L., Nennig E., Stippich C., "Effects of covert and overt paradigms in clinical language fMRI", *Acad Radiol* **19,** 518-525 (2012).
[128] Pauling L., Coryell C. D., "The Magnetic properties and structure of hemoglobin, oxyhemoglobin and carbonmonoxyhemoglobin", *Proc Natl Acad Sci U S A* **22,** 210-216 (1936).
[129] Pavlova E., Kuo M. F., Nitsche M. A., Borg J., "Transcranial direct current stimulation of the premotor cortex: effects on hand dexterity", *Brain Res* **1576,** 52-62 (2014).
[130] Penfield W., Rasmussen T., *The cerebral cortex of man*. New York: Macmillan Company, 1950.
[131] Picht T., Krieg S. M., Sollmann N., Rosler J., Niraula B., Neuvonen T., Savolainen P., Lioumis P., Mäkelä J. P., Deletis V., Meyer B., Vajkoczy P., Ringel F., "A comparison of language mapping by preoperative navigated transcranial magnetic stimulation and direct cortical stimulation during awake surgery", *Neurosurgery* **72,** 808-819 (2013).
[132] Picht T., Mularski S., Kuehn B., Vajkoczy P., Kombos T., Suess O., "Navigated transcranial magnetic stimulation for preoperative functional diagnostics in brain tumor surgery", *Neurosurgery* **65,** 93-98; discussion 98-99 (2009).
[133] Picht T., Schmidt S., Brandt S., Frey D., Hannula H., Neuvonen T., Karhu J., Vajkoczy P., Suess O., "Preoperative functional mapping for rolandic brain tumor surgery: comparison of navigated transcranial magnetic stimulation to direct cortical stimulation", *Neurosurgery* **69,** 581-588; discussion 588 (2011).
[134] Plautz E. J., Milliken G. W., Nudo R. J., "Effects of repetitive motor training on movement representations in adult squirrel monkeys: role of use versus learning", *Neurobiol Learn Mem* **74,** 27-55. (2000).

[135] Poldrack R. A., "Region of interest analysis for fMRI", *Soc Cogn Affect Neurosci* **2,** 67-70 (2007).
[136] Prekeges J., *Nuclear medicine instrumentation*. Sudbury: Jones and Bartlett Publishers, LLC, 211.
[137] Purcell E. M., Torrey H. C., Pound R. V., "Resonance absorption by nuclear magnetic moments in solid", *Phys Rev* **69,** 37-38 (1946).
[138] Rademacher J., Burgel U., Geyer S., Schormann T., Schleicher A., Freund H. J., Zilles K., "Variability and asymmetry in the human precentral motor system. A cytoarchitectonic and myeloarchitectonic brain mapping study", *Brain* **124,** 2232-2258 (2001).
[139] Raichle M. E., "Behind the scenes of functional brain imaging: a historical and physiological perspective", *Proc Natl Acad Sci U S A* **95,** 765-772 (1998).
[140] Rossini P. M., Barker A. T., Berardelli A., Caramia M. D., Caruso G., Cracco R. Q., Dimitrijevic M. R., Hallett M., Katayama Y., Lucking C. H., et al., "Non-invasive electrical and magnetic stimulation of the brain, spinal cord and roots: basic principles and procedures for routine clinical application. Report of an IFCN committee", *Electroencephalogr Clin Neurophysiol* **91,** 79-92 (1994).
[141] Roth B. J., Basser P. J., "A model of the stimulation of a nerve fiber by electromagnetic induction", *IEEE Trans Biomed Eng* **37,** 588-597 (1990).
[142] Ruohonen J., Ilmoniemi R. Basic physics and design of transcranial magnetic stimulation devices and coils. In: Hallet M., Chokroverty S., eds. *Magnetic stimulation in clinical neurophysiology*. 2nd edn. Philadelphia: Elsevier, 2005: 17-30.
[143] Ruohonen J., Ilmoniemi R. J., "Modeling of the stimulating field generation in TMS", *Electroencephalogr Clin Neurophysiol Suppl* **51,** 30-40 (1999).
[144] Säisänen L., Julkunen P., Niskanen E., Danner N., Hukkanen T., Lohioja T., Nurkkala J., Mervaala E., Karhu J., Könönen M., "Motor potentials evoked by navigated transcranial magnetic stimulation in healthy subjects", *J Clin Neurophysiol* **25,** 367-372 (2008).
[145] Sandbrink F. The MEP in clinical neurodiagnosis. In: Wassermann E. M., Epstein C. M., Ziemann U., Walsh V., Paus T.,

Lisanby S. H., eds. *The Oxford Handbook of Transcranial Stimulation*. New York: Oxford University Press, 2008: 237-283.

[146] Schaechter J. D., "Motor rehabilitation and brain plasticity after hemiparetic stroke", *Prog Neurobiol* **73,** 61-72 (2004).

[147] Schenck J. F., "The role of magnetic susceptibility in magnetic resonance imaging: MRI magnetic compatibility of the first and second kinds", *Med Phys* **23,** 815-850 (1996).

[148] Schieber M. H. Voluntary descending control. In: Zigmond L. M., Bloom F. E., Landis S. E., Roberts J. L., Squire L. R., eds. *Fundamental Neuroscience*. London: Academic Press, 1999: 931-949.

[149] Schreckenberger M., Spetzger U., Sabri O., Meyer P. T., Zeggel T., Zimny M., Gilsbach J., Buell U., "Localisation of motor areas in brain tumour patients: a comparison of preoperative [18F]FDG-PET and intraoperative cortical electrostimulation", *Eur J Nucl Med* **28,** 1394-1403 (2001).

[150] Simonyan K., Fuertinger S., "Speech networks at rest and in action: interactions between functional brain networks controlling speech production", *J Neurophysiol* **113,** 2967-2978 (2015).

[151] Sladky R., Friston K. J., Trostl J., Cunnington R., Moser E., Windischberger C., "Slice-timing effects and their correction in functional MRI", *Neuroimage* **58,** 588-594 (2011).

[152] Sollmann N., Ille S., Hauck T., Maurer S., Negwer C., Zimmer C., Ringel F., Meyer B., Krieg S. M., "The impact of preoperative language mapping by repetitive navigated transcranial magnetic stimulation on the clinical course of brain tumor patients", *BMC Cancer* **15,** 261

[153] Sollmann N., Picht T., Makela J. P., Meyer B., Ringel F., Krieg S. M., "Navigated transcranial magnetic stimulation for preoperative language mapping in a patient with a left frontoopercular glioblastoma", *J Neurosurg* **118,** 175-179 (2013).

[154] Sollmann N., Tanigawa N., Ringel F., Zimmer C., Meyer B., Krieg S. M., "Language and its right-hemispheric distribution in healthy brains: an investigation by repetitive transcranial magnetic stimulation", *Neuroimage* **102,** 776-788 (2014).

[155] Sollmann N., Tanigawa N., Tussis L., Hauck T., Ille S., Maurer S., Negwer C., Zimmer C., Ringel F., Meyer B., Krieg S. M., "Cortical regions involved in semantic processing investigated by

repetitive navigated transcranial magnetic stimulation and object naming", *Neuropsychologia* **70,** 185-195 (2015).

[156] Speck O., Hennig J., Zaitsev M., "Prospective real-time slice-by-slice motion correction for fMRI in freely moving subjects", *Magma* **19,** 55-61 (2006).

[157] Spector R., Robert Snodgrass S., Johanson C. E., "A balanced view of the cerebrospinal fluid composition and functions: Focus on adult humans", *Exp Neurol* **273,** 57-68 (2015).

[158] Stewart L., Walsh V., Frith U., Rothwell J. C., "TMS produces two dissociable types of speech disruption", *Neuroimage* **13,** 472-478 (2001).

[159] Stippich C., Rapps N., Dreyhaupt J., Durst A., Kress B., Nennig E., Tronnier V. M., Sartor K., "Localizing and lateralizing language in patients with brain tumors: feasibility of routine preoperative functional MR imaging in 81 consecutive patients", *Radiology* **243,** 828-836 (2007).

[160] Sunaert S., "Presurgical planning for tumor resectioning", *J Magn Reson Imaging* **23,** 887-905 (2006).

[161] Szelenyi A., Bello L., Duffau H., Fava E., Feigl G. C., Galanda M., Neuloh G., Signorelli F., Sala F., "Intraoperative electrical stimulation in awake craniotomy: methodological aspects of current practice", *Neurosurg Focus* **28,** E7 (2010).

[162] Takeuchi N., Izumi S., "Rehabilitation with poststroke motor recovery: a review with a focus on neural plasticity", *Stroke Res Treat* **2013,** 128641 (2013).

[163] Talairach J., Tournoux P., *Co-planar Stereotaxic Atlas of the Human Brain: 3-Dimensional Proportional System - an Approach to Cerebral Imaging*. New York: Thieme Medical Publishers, 1988.

[164] Tanaka F., Vines D., Tsuchida T., Freedman M., Ichise M., "Normal patterns on 99mTc-ECD brain SPECT scans in adults", *J Nucl Med* **41,** 1456-1464 (2000).

[165] Taub E., Crago J. E., Burgio L. D., Groomes T. E., Cook E. W., 3rd, DeLuca S. C., Miller N. E., "An operant approach to rehabilitation medicine: overcoming learned nonuse by shaping", *J Exp Anal Behav* **61,** 281-293. (1994).

[166] Taub E., J.E. C., Uswatte G., "Constraint-Induced Movement Therapy: A new approach to treatment in physical rehabilitation", *Rehabilitation Psychilogy* **43,** 152-170 (1998).

[167] Taub E., Miller N. E., Novack T. A., Cook E. W., 3rd, Fleming W. C., Nepomuceno C. S., Connell J. S., Crago J. E., "Technique to improve chronic motor deficit after stroke", *Arch Phys Med Rehabil* **74,** 347-354. (1993).

[168] Taub E., Uswatte G., Pidikiti R., "Constraint-Induced Movement Therapy: a new family of techniques with broad application to physical rehabilitation--a clinical review", *J Rehabil Res Dev* **36,** 237-251. (1999).

[169] Taussig D., Montavont A., Isnard J., "Invasive EEG explorations", *Neurophysiol Clin* **45,** 113-119 (2014).

[170] Taylor J. L., Gandevia S. C., "Noninvasive stimulation of the human corticospinal tract", *J Appl Physiol* **96,** 1496-1503 (2004).

[171] Thesen S., Heid O., Mueller E., Schad L. R., "Prospective acquisition correction for head motion with image-based tracking for real-time fMRI", *Magn Reson Med* **44,** 457-465 (2000).

[172] Thickbroom G. W., Byrnes M. L., Sacco P., Ghosh S., Morris I. T., Mastaglia F. L., "The role of the supplementary motor area in externally timed movement: the influence of predictability of movement timing", *Brain Res* **874,** 233-241 (2000).

[173] van den Heuvel M. P., Hulshoff Pol H. E., "Exploring the brain network: a review on resting-state fMRI functional connectivity", *Eur Neuropsychopharmacol* **20,** 519-534 (2010).

[174] van Eijndhoven P., van Wingen G., Fernandez G., Rijpkema M., Pop-Purceleanu M., Verkes R. J., Buitelaar J., Tendolkar I., "Neural basis of recollection in first-episode major depression", *Hum Brain Mapp* **34,** 283-294 (2013).

[175] van Heerden J., Desmond P. M., Phal P. M., "Functional MRI in clinical practice: a pictorial essay", *J Med Imaging Radiat Oncol* **58,** 320-326 (2014).

[176] Van Laere K., Versijpt J., Audenaert K., Koole M., Goethals I., Achten E., Dierckx R., "99mTc-ECD brain perfusion SPET: variability, asymmetry and effects of age and gender in healthy adults", *Eur J Nucl Med* **28,** 873-887 (2001).

[177] Veerbeek J. M., van Wegen E., van Peppen R., van der Wees P. J., Hendriks E., Rietberg M., Kwakkel G., "What is the evidence for physical therapy poststroke? A systematic review and meta-analysis", *PLoS One* **9,** e87987 (2014).

[178] Visani E., Agazzi P., Canafoglia L., Panzica F., Ciano C., Scaioli V., Avanzini G., Franceschetti S., "Movement-related desynchronization-synchronization (ERD/ERS) in patients with Unverricht-Lundborg disease", *Neuroimage* **33,** 161-168 (2006).

[179] Visani E., Canafoglia L., Gilioli I., Sebastiano D. R., Contarino V. E., Duran D., Panzica F., Cubeddu R., Contini D., Zucchelli L., Spinelli L., Caffini M., Molteni E., Bianchi A. M., Cerutti S., Franceschetti S., Torricelli A., "Hemodynamic and EEG Time-courses during unilateral hand movement in patients with cortical myoclonus. An EEG-fMRI and EEG-TD-fNIRS study", *Brain Topogr* (2014).

[180] Wada T., Ohnuma T., Ohsawa T., "Eeg Studies on Cerebral Circulatory Disturbances in Man. I. Results Due to Carotid Compression Test", *Seishin Shinkeigaku Zasshi* **17,** 113-128 (1963).

[181] Ward H. A., Riederer S. J., Grimm R. C., Ehman R. L., Felmlee J. P., Jack C. R., Jr., "Prospective multiaxial motion correction for fMRI", *Magn Reson Med* **43,** 459-469 (2000).

[182] Ward N. S., "Functional reorganization of the cerebral motor system after stroke", *Curr Opin Neurol* **17,** 725-730 (2004).

[183] Weisskoff R. M., Kiihne S., "MRI susceptometry: image-based measurement of absolute susceptibility of MR contrast agents and human blood", *Magn Reson Med* **24,** 375-383 (1992).

[184] Wengenroth M., Blatow M., Guenther J., Akbar M., Tronnier V. M., Stippich C., "Diagnostic benefits of presurgical fMRI in patients with brain tumours in the primary sensorimotor cortex", *Eur Radiol* **21,** 1517-1525 (2011).

[185] Wernicke C., *Der aphasische Symptomenkomplex*: Breslau: M. Cohn und Weigert, 1874.

[186] Winstein C. J., Grafton S. T., Pohl P. S., "Motor task difficulty and brain activity: investigation of goal-directed reciprocal aiming using positron emission tomography", *J Neurophysiol* **77,** 1581-1594. (1997).

[187] Wolf S. L., Lecraw D. E., Barton L. A., Jann B. B., "Forced use of hemiplegic upper extremities to reverse the effect of learned nonuse among chronic stroke and head-injured patients", *Exp Neurol* **104,** 125-132. (1989).

[188] Wolf S. L., Winstein C. J., Miller J. P., Taub E., Uswatte G., Morris D., Giuliani C., Light K. E., Nichols-Larsen D., "Effect of

constraint-induced movement therapy on upper extremity function 3 to 9 months after stroke: the EXCITE randomized clinical trial", *Jama* **296,** 2095-2104 (2006).

[189] Wolf T., Lindauer U., Villringer A., Dirnagl U., "Excessive oxygen or glucose supply does not alter the blood flow response to somatosensory stimulation or spreading depression in rats", *Brain Res* **761,** 290-299 (1997).

[190] Worsley K. J., Friston K. J., "Analysis of fMRI time-series revisited--again", *Neuroimage* **2,** 173-181 (1995).

[191] Yesilyurt B., Ugurbil K., Uludag K., "Dynamics and nonlinearities of the BOLD response at very short stimulus durations", *Magn Reson Imaging* **26,** 853-862 (2008).

[192] Yip P. K., Jeng J. S., Lee T. K., Chang Y. C., Huang Z. S., Ng S. K., Chen R. C., "Subtypes of ischemic stroke. A hospital-based stroke registry in Taiwan (SCAN-IV)", *Stroke* **28,** 2507-2512 (1997).

[193] Yousry T. A., Schmid U. D., Alkadhi H., Schmidt D., Peraud A., Buettner A., Winkler P., "Localization of the motor hand area to a knob on the precentral gyrus. A new landmark", *Brain* **120 (Pt 1),** 141-157 (1997).

[194] Zaca D., Jarso S., Pillai J. J., "Role of semantic paradigms for optimization of language mapping in clinical FMRI studies", *AJNR Am J Neuroradiol* **34,** 1966-1971 (2013).

[195] Ziemann U. TMS measures of motor cortical and corticospinal excitability: Physiology, function and plasticity. In: Wassermann E. M., Epstein C. M., Ziemann U., Walsh V., Paus T., Lisanby S. H., eds. *The Oxford Handbook of Transcranial Stimulation*. New York: Oxford University Press, 2008: 75-234.

Mervi Könönen

Functional Human Neuroimaging Using Clinical Tools

Studies of Cortical Motor Areas

Neuroimaging tools can be used to study the structures and functions of the brain, and to localize these functions. In this thesis, single photon emission tomography, functional magnetic resonance imaging and transcranial magnetic stimulation were shown to be able to identify functional changes related to motor performance. Additionally, by using a multimodal approach, it was possible to discern the brain areas responsible to motor and language processes involved in overt speech production.

UNIVERSITY OF
EASTERN FINLAND

Publications of the University of Eastern Finland
Dissertations in Forestry and Natural Sciences

ISBN: 978-952-61-1153-7 (printed)
ISSN: 1798-5668
ISBN: 978-952-61-1154-4 (pdf)
ISSN: 1798-5676 (pdf)